Journal of Visualized Experiments

Fixed target serial data collection at Diamond Light Source

--Manuscript Draft--

Article Type:	Methods Article - Author Produced Video
Manuscript Number:	JoVE62200R1
Full Title:	Fixed target serial data collection at Diamond Light Source
Corresponding Author:	Robin Owen Diamond Light Source Didcot, Oxfordshire UNITED KINGDOM
Corresponding Author's Institution:	Diamond Light Source
Corresponding Author E-Mail:	robin.owen@diamond.ac.uk
Order of Authors:	Sam Horrell, Ph.D
	Danny Axford
	Nicholas Devenish
	Ali Ebrahim
	Michael Hough
	Darren Sherrell
	Selina Storm
	Ivo Tews
	Jonathan Worrall
	Robin Owen
Additional Information:	
Question	**Response**
Please indicate whether this article will be Standard Access or Open Access.	Open Access (US$4,200)
Please indicate the **city, state/province, and country** where this article will be **filmed**. Please do not use abbreviations.	Oxford, England, UK
Please specify the section of the submitted manuscript.	Biochemistry
Please confirm that you have read and agree to the terms and conditions of the author license agreement that applies below:	I agree to the Author License Agreement
Please provide any comments to the journal here.	
Please indicate whether this article will be Standard Access or Open Access.	Open Access (US$3000)

TITLE:

Fixed target serial data collection at Diamond Light Source

AUTHORS AND AFFILIATIONS:

Sam Horrell[1], Danny Axford[1], Nicholas E. Devenish[1], Ali Ebrahim[1], Michael A. Hough[2], Darren A. Sherrell[1], Selina L. S. Storm[1], Ivo Tews[3], Jonathan. A. R. Worrall[2], Robin L. Owen[1]*

1. Diamond Light Source, Harwell Science and Innovation Campus, Didcot, Oxfordshire, UK
2. School of Life Sciences, University of Essex, Wivenhoe Park, Colchester, UK
3. Biological Sciences, Institute for Life Sciences, University of Southampton, Highfield Campus, Southampton, United Kingdom

sam.horrell@diamond.ac.uk
danny.axford@diamond.ac.uk
nicholas.devenish@diamond.ac.uk
ali.ebrahim@diamond.ac.uk
mahough@essex.ac.uk
dsherrell@anl.gov
selina.storm@diamond.ac.uk
ivo.tews@soton.ac.uk
jworrall@essex.ac.uk
robin.owen@diamond.ac.uk

* Corresponding Author

KEYWORDS:

Serial Crystallography, Structural Biology, Macromolecular crystallography

SUMMARY:

We present a comprehensive guide to fixed target sample preparation, data collection, and data processing for serial synchrotron crystallography at Diamond beamline I24.

ABSTRACT:

Serial data collection is a relatively new technique for synchrotron users. A user manual for fixed target data collection at I24, Diamond Light Source is presented with detailed step-by-step instructions, Figures, and videos for smooth data collection.

INTRODUCTION:

Serial synchrotron crystallography (SSX) is an emerging method of data collection which was inspired by X-ray free electron lasers (XFEL)[1-3]. At an XFEL, a single diffraction pattern is recorded from a usually very small, protein crystal before the crystal is destroyed by the extremely bright X-ray pulse. This means, typically, that a new crystal must be introduced into the X-ray beam to obtain another diffraction pattern[4]. This need to continually replenish crystals has driven the development of many serial sample delivery techniques[5].

At synchrotrons, classic (non-serial) rotation crystallography methods are widely applied, exploiting a single large crystal which is rotated in an X-ray beam using a goniometer to collect a complete dataset for structure solution[6]. In order to increase the lifetime of crystals so that a complete dataset can be collected[7,8], and also to facilitate shipping and automated sample transfer, crystals are cryocooled to ~100 K for data collection. At intense microfocus beamlines, multi-crystal strategies are frequently employed as radiation damage can prohibit the collection of a complete dataset from a single crystal[9-11]. Despite the limits imposed by radiation damage, the number of crystals used remains relatively modest and the approach used is essentially identical to the single crystal experiment.

SSX, on the other hand, uses serial sample delivery to obtain single still diffraction patterns from thousands of randomly orientated crystals to generate a complete dataset. It is noted that serial techniques incorporating crystal rotation are under development[12-13] though we focus on still, zero rotation, approaches. There are a wide variety of sample delivery systems with different advantages and disadvantages[14], ranging from delivering a stream of crystals in a flow focused/viscous jet[15-17], microfluidic chip[18-19], or crystals on a fixed target such as an etched silicon chip[20-21]. Typically, crystals are held at room temperature, allowing greater conformational diversity to be observed and providing a more physiologically relevant environment[22]. SSX enables the collection of very low dose datasets[23], as the total dose of the dataset is equivalent to a single short X-ray exposure of one crystal. Another major advantage SSX provides is the study protein dynamics through time-resolved methods, with reactions triggered by exposure to laser light[24-27] or by mixing of crystals and ligand/substrate[28-29]. Using smaller crystals means laser light can penetrate the entirety of the crystal, uniformly initiating the reaction without multiphoton absorption to provide well defined reaction intermediates for diffraction data taken at different time points[27]. Use of larger crystals and rotation-based data collection methods suffers from a limited laser penetration depth, nonuniform or multiphoton activation, radiation damage, and mechanical overhead time within data sweeps, resulting in a mix of reaction intermediates that can prove difficult or impossible to interpret at faster reaction speeds. Smaller crystals provide a similar advantage in mixing experiments, as ligands can rapidly and more uniformly diffuse throughout the crystal, again allowing defined reaction intermediates to be recorded at different time delays[30-32].

At Diamond's microfocus beamline I24 both conventional rotation and SSX experiments can be performed. Here a comprehensive protocol for SSX sample preparation and data collection using fixed targets at I24 and protocols for data analysis of serial data at Diamond are presented. While the manuscript and accompanying videos should allow users to carry out a successful SSX experiment at I24, it should be noted that this is a rapidly developing field and approaches are continually evolving. It should also be noted that serial methods are available at other synchrotron sources, including but not limited to Petra III (P14-TREXX), MAX IV (BioMAX)[33], SLS (PXI and PXII)[34], and NSLS (FMX)[35], and that the specifics of serial data collection and processing will differ but the core principles will remain the same. The protocols below should be seen to represent a starting point and a pathway to base camp rather than the summit of what might be achieved.

This protocol assumes the users have a protein or small molecule crystal system, from which a microcrystal slurry on the order of 0.5-2.0 mL with a good density of microcrystals per mL has been produced. Protocols for obtaining crystal slurries are described in [36]. Many different types of fixed target are available, the most commonly used at I24 utilize a precisely defined silicon chip. In order to differentiate from other chip layouts, below and in the beamline interface this is referred to as an 'Oxford chip'. As previously described the Oxford chip layout comprises 8×8 'city blocks', each containing 20×20 apertures for a total of 25,600 apertures[20-21].

PROTOCOL:

1. Preparing and loading a chip

NOTE: The process occurs within a humidity-controlled environment (**Figure 1**), typically 80% or higher relative humidity, to prevent protein crystals from drying out. Once loaded and sealed, crystals can survive for upwards of 24 hours. However, this is can vary greatly between crystal systems. Within the chamber a low powered vacuum pump attached to a loading stage to hold a silicon chip (**Figure 1**), a silicon chip, a chip holder with polyester foil (**Figure 2**), a p200 pipette, 200 µL pipette tips, tweezers, filter paper and the protein crystal slurry are required.

1.1 Prepare a chip holder.

1.1.1 Cut two sheets of polyester foil into squares approximately 6 cm x 6 cm.

1.1.2 Lay the polyester sheets over the two base plates (large and small).

1.1.3 Fix the polyester sheets in place using the metal sealing rings.

1.1.4 Carefully pull on the excess polyester foil to remove any creases to make visualizing and centering samples easier later.

1.2 Select a silicon chip with appropriately sized apertures (7-30 µm) relative to the size of the crystals.

1.3 Glow discharge the chip for 25 seconds at 0.39 mBar and using a current of 15 mA to enable easy spreading of micro crystals on the chip.

1.4 Place the silicon chip on the chip loading stage using tweezers with the raised bars facing down.

1.5 Apply 200 µL of the micro-crystal slurry to the flat side of the chip using a pipette.

1.6 Spread out the crystal slurry to cover all the "city-blocks" of the chip.

1.7 If the chip is damaged, cover any holes with a small piece of polyester foil or filter pipette tip to ensure an even vacuum can be applied.

1.8 Apply a gentle vacuum until all excess liquid has been sucked through the chip.

1.9 Remove the chip from the chip loading stage with tweezers.

1.10 Carefully blot the underside of the chip with filter paper to remove excess liquid.

1.11 Place the loaded chip on the larger half of the chip holder between the guide marks flat side down.

1.12 Seal the chip by placing the small half of the chip holder on top.

1.12.1 The two halves of the chip holder will snap into place. If the second half does not sit flush, spin the holder 180° to properly align the magnets.

1.13 Screw the chip holder closed with hex bolts to fix the chip securely in place.

NOTE: Alternatively, a "chipless" chip can be loaded in a similar fashion, with a smaller volume of crystal slurry (~15 µL) sandwiched between the two layers of polyester foil in the chip holder [37], or a smaller volume can be loaded using a 50 µm thick double-sided adhesive spacer applied directly to the polyester foil as described in [38]. The use of adhesive spacers also allows multiple samples (or variants of samples such as ligand soaks) to be loaded on each chipless chip. A complementary loading approach exploiting acoustic drop ejection (ADE) to load silicon chips can also be used at Diamond[39]. ADE allows chips to be loaded using smaller volumes of crystal slurry than pipette loading. It is a particularly useful technique when samples are scarce, though the chemical composition and viscosity of the slurry must be taken into consideration.

2 GUI and setup at the beamline

±

2.1 Perform all chip alignment and setup for data collection through a simple EPICS Display Manager (edm) graphical user interface (GUI) (**Figure 3a**). This provides a point and click interface to beamline instrumentation and provides input parameters for python-based data collection. Sub windows provide additional control for collecting from sub regions of a sample holder (**Figure 3b**) or laser/LED pump-probe experiments (**Figure 3c**).

3 Aligning the chip

3.1 Place the loaded chip on the XYZ stage at the beamline (shown in **Figure 4a**) using the kinematic mounts.

3.1.1 Take care to avoid pulling the stages along their direction of travel. The magnets in the kinematic mounts are quite strong so this can be done quite easily by accident.

3.1.2 When approaching the mount, the chip holder should be held at a slight angle (±30°). When the magnets make contact allow the chip holder to rotate parallel to the flow (0°) and the chip holder will click into place (**Figure 4b**).

3.1.3 When unloading a chip follow a reverse path. Rotate and angle the chip away from the stages before pulling the chip holder away.

3.2 Using the beamline's on-axis viewing system and the chip alignment GUI, locate the top left fiducial of the chip. Fiducials are three squares, two small and one large, at right angles to one another (**Figure 5a**). The chip is back illuminated so the chip will appear dark with apertures as white squares.

3.3 Center on fiducial zero in X, Y, and Z (**Figure 5b**). Align X and Y by moving left/right and up/down, respectively. Align Z by moving the chip in and out of focus.

3.4 Click **Set Fiducial Zero**.

3.5 Repeat step 3.2 for fiducial one (top right, **Figure 5c**) and fiducial two (bottom left, **Figure 5d**) to align all fiducials with the X-ray beam.

3.6 Generate a co-ordinate matrix by pressing 'make co-ordinate system', this calculates the offset, pitch, roll, and yaw of the chip relative to the stages allowing all subsequent movements to be done in the chip co-ordinate frame.

3.7 Click **Block Check** to move the XYZ stage to the first well of each city block for visual confirmation that the chip is well aligned.

3.8 If the X-ray crosshair lines up with the apertures the chip is aligned. If not, repeat steps 3.2-3.3.

NOTES: In case of difficulty aligning (broken fiducials), different apertures on the chip can be used for alignment using the "alignment type" pull-down menu. Many different types of chip are available for fixed target data collection. Different chip types are accommodated through use of the 'chip type' pull-down menu. The most common chip types used at I24 are 'Oxford' and 'custom' chips. The number and the spacing of apertures and fiducials on the chip are read from a chip dictionary defined *via* the pull-down menu. Custom chip allows the aperture spacing to be defined on-the-fly, which is particularly useful for thin-film sheet-on-sheet or other 'chipless' type chips where crystals are randomly located across the holder[37]. A new python GUI, offering move-on-click functionality and automated chip alignment is currently under development, but is not yet ready for routine use at the time of the writing of this manuscript.

4 Setting up data collection

NOTE: Data collection setup will depend on the system being studied, and the experiment to be performed. This can range from the simplest SSX experiment, collecting a low dose structure, to a time-resolved experiment using lasers or rapid mixing to initiate a reaction which will require multiple complete datasets at different time delays. To set up a data collection the following parameters need to be defined.

4.1 Experimental variables: Fill in the Folder, filename, exposure time, transmission, detector distance, and number of shots per aperture in as appropriate.

4.2 Chip type: As described above, match the chip type to the chip in use.

4.2.1 If a thin film or 'chipless' chip is being used, then set the chip type to **None**.

4.2.2 Define the number of steps and step size in both x and y in the GUI.

4.3 Set the map type: this allows subsections of a chip to be selected for data collection (**Figure 3b**). 'None' means data are collected from every aperture on a chip. 'Lite' means data are collected from selected city blocks on the chip (**Figure 3b**). This can be useful if, for example, a region of a chip is known to be poorly loaded or empty. 'Full' allows individual apertures to be selected for data collection. In this case a correctly formatted text file must be provided.

4.4 Pump-probe: Select the type of pump probe experiment and the desired time delay. The triggering of the pump (usually a LED or laser) is often specific to a particular experiment, so will not be described in detail here.

4.4.1 'Short' delays refer to experiments when there is a dwell at each aperture between the pump and the probe (i.e., pump, probe, move to the next sample.) Delays are typically on the order of 1 second or tens of milliseconds.

4.4.2 'Long' delays refer to an excite and visit again (EAVA) strategy, where apertures are visited twice, with a defined time delay between visits (i.e., pump, move, pump, move, probe, move, probe, etc.). Calculate the time delay based on the requested laser and X-ray exposure times (**Figure 3c**) and it is typically ~1 second or more.

5 Common data collection methods

NOTE: The following are the key parameters that define the type of experiment being carried out. This section assumes that the other settings from protocol 3 "Setting up Data Collection" have been defined.

5.1 **Scenario 1**: Low-dose data collection. Collection of a single diffraction image from every selected aperture on the sample holder.

5.1.1 Set number of shots per aperture to 1.

5.1.2 Set pump probe to **None**.

5.2 **Scenario 2**: A dose series, collecting *n* images sequentially from every selected aperture on the sample holder. The chip is stationary at each aperture while each set of *n* images is collected.

5.2.1 Set the number of shots per aperture to '*n*'. Note that processing is simplified if *n*=5, 10, 20 or another multiple of 10. It is difficult to establish trends if n < 5. It is useful to consider the total time required to cover a chip and the number of image files produced when *n* is increased.

5.2.2 Set pump probe to **None**.

5.3 **Scenario 3**: Pump-probe methods

5.3.1 Select a method from the **Pump Probe** pull-down menu to open the Laser Excitation Control Centre.

5.3.2 For a pump probe experiment fill in the **Laser Dwell at each aperture** option.

5.3.3 For EAVA fill in the **Laser Dwell at each aperture** and **X-ray exposure** and click **Calculate**.

5.3.4 Select the appropriate **Repeat** option in the edm GUI pump probe drop-down menu for the desired delay time.

5.3.5 If the experiment requires a pre-illumination step fill in the **Laser 2 Dwell** section.

5.3.6 After all experimental variables are defined press **Set parameters and create short list**. This loads experimental variables onto the geobrick controller. After this is done pressing **Start** will move the detector in, the backlight out, and start data collection. At all points in setting up data collection it is useful to have a terminal window open where feedback on the status and outcome of each of the steps is printed.

6 Data processing

NOTE: Broadly speaking data processing can be divided into three groups based on the urgency with which feedback is required. Fast feedback is required to show if crystals are present and diffract, and if so, in what numbers. This should keep up with data collection. Performing data indexing and integration which can be slower but should still be performed on comparable time scales with data collection. Merging and scaling of reflection intensities into an mtz file for structure solution and the generation of electron density maps represents the final step and can be slower still. Here starting pipelines at I24 for the first two stages only will be discussed, as they are required for real-time feedback to guide your experiment, though note that metrics such as

hit-rates and scaling statistics are not a substitute for inspecting electron density, which may provide the only confirmation that a ligand has bound, or a reaction occurred, *in crystallo*.

6.1 Fast feedback

6.1.1 To load the data processing modules type **module load i24-ssx** into the terminal on any beamline workstation.

6.1.2 To run the hit-finding analysis type **i24-ssx /path/to/visit/directory/** into the terminal: i24-ssx /dls/i24/data/2020/mx12345-6/

NOTE: This opens three terminal windows and, once data has been written to disk, a graphical representation of spot finding results from Diffraction Integration for Advanced Light Sources (DIALS) [40-41] (**Figure 6a**).

6.1.2.1.1 Default settings scores every 10th image and refreshes every few seconds to minimise the computational load.

6.1.2.1.2 Change the default by adding an argument to the end of the command above. For example, 'i24-ssx /dls/i24/data/2020/mx12345-6 2' i24-ssx would run hit finding on every other image. However, this can put undue strain on the cluster (a shared resource!) and slow down processing times. The graph is color coded based on the likelihood of successful indexing, red shows at least 15 Bragg spots have been found (good chance of indexing), blue shows little to no useful diffraction.

6.1.2.1.3 View diffraction images of interest in the DIALS image viewer by clicking on the spots on the spot finder interface.

6.2 Indexing and integration feedback

NOTE: Indexing and integration of diffraction data are performed with DIALS using the dials.still_process function [40-41]. As such, specific information relating to your crystal (expected crystal space group, unit cell, and an experiment geometry) should be put into a .phil text file.

6.2.1 Load DIALS modules by typing **module load dials** in a terminal.

6.2.2 To begin processing a dataset type **dials.still_process /path/to/images/ /pathto/phil-file.phil.** The progress of all still processing datasets can be monitored by running the **stills_monitor** script by typing **monitor_stills_process.py** (after performing module load i24-ssx and changing directory to the current visit) (**Figure 6b**).

6.2.3 Moniotr the unit cell distribution of indexed diffraction data (**Figure 7a**) can be monitored using the command **ctbx.xfel.plot_uc_cloud_from_experiments/path/to/dials/output/*refined.expt**

combine_all_input=true This is particularly useful to identify and resolve unit cell polymorphs as seen in [42].

6.2.4 Visualzie if, and how, this distribution varies across a fixed target by producing a 2D plot (**Figure 7b**) using the command **python pacman.py /visit/processing/_hit_finding/chip.out**.

6.2.5 Produce stereographic projections of all indexed diffraction data (**Figure 7c**) using the DIALS command **dials.stereographic_projection hkl=0,0,1 expand_to_P1=True /path/to/dials/output/*refined.expt.**

NOTE: It is a common pathology when processing stills data from crystals where the symmetry of the Bravais lattice is higher than the space group symmetry that merged data appear as a perfect twin. Data processing algorithms have evolved to resolve this pathology [43-46] but users should be mindful of this while processing their data.

REPRESENTATIVE RESULTS:

Low Dose Data Collection and Series

Low dose (Step 5.1: Scenario 1) and dose series (Step 5.2: Scenario 2) data were collected on copper nitrite reductase micro crystals at I24 and have been published in [42]. All samples were prepared as described in step 1, data collected as per steps 3, 4, and 5, and processed using methods in step 6. In this work a rapid dose series was collected with 20 diffraction images taken at each aperture (i.e., *n*=20 in the data collection GUI shown above) before moving to fresh sample. From these data a bimodal distribution of unit cells in space group $P2_13$ was identified (a = b = c = 97.25 Å, and a = b = c = 96.38 Å). Identifying and separating these unit-cell polymorphs for processing showed a marked improvement in data quality indicators and revealed two different structures in a flexible loop between residues 189-193 instead of the mixed state observed when processing all data together. Identification of such polymorphs could make all the difference in a delicate time-resolved structural study where only small structural changes are expected. Furthermore, the dose series collected revealed a dose dependent unit cell change in the crystal, with increased dose shifting the population in favor of the larger unit-cell.

Similar work was performed in[47], where a dose series (Step 5.2: Scenario 2) was collected from a dye-type heme peroxidase from *Streptomyces lividans* (DtpAa) to compare low dose structures from SSX (Step 5.1: Scenario 1) with those measured in the same fixed target system using SFX. SFX data were collected at SACLA Beamline BL2 EH3 with a pulse length of 10 femtoseconds and a repetition rate of 30 Hz. The 10 femtosecond pulse duration ensures that dose dependent effects are not present in the SFX data. SFX data were compared to SSX data collected on beamline I24, where 10 sequential 10 millisecond exposures were measured at each sample position (i.e., *n*=10). The dose dependent migration of a heme iron coordinated water molecule away from the iron was observed, as well as a conformational change in one of the heme propionate groups in the SSX dose series. Although not damage-free like the SFX structure, the dose series allowed the Fe-O_2H bond length of a zero-dose dataset (ferric heme) to be extrapolated, with this agreeing within experimental error with the value obtained from SFX.

The serial crystallography data collection methods described here can also be easily adapted to provide new sample environments to, for example, study anaerobic protein structures at room temperature. As outlined in [48], loading a 'sheet-on-sheet' sample, or 'chipless chip', with different sealing films in an anerobic chamber enables room temperature collection of structural data from dioxygen-sensitive samples.

Pump Probe

Although the following representative results were not collected at Diamond Beamline I24, these methods have been developed in close collaboration between facilities in the iNEXT program to work towards standard methods in serial crystallography method development. Beamline I24 offers, or will soon offer, equivalent collection methods to those used below already in the literature to perform such experiments using the methods described in the protocols above.

Pump Probe: Rapid Mixing

Rapid mixing SSX has been performed at beamline TREXX at PETRA III by [28] using a piezo driven droplet injector to initiate reactions on fixed targets. This work presents a proof of principle on chip mixing experiment binding $GlcNac_3$ to lysozyme microcrystals, with binding occurring within 50 ms of a 75 pL drop being applied to the sample. This study was followed up with a 7-structure time-resolved series of xylose isomerase activity, demonstrating glucose binding within 15 ms and the formation of an open ring conformation in the glucose molecule after a 60 second time delay. An equivalent setup for droplet injection is currently under development for use on I24.

Pump-Probe: Light Activation

A light activated pump-probe serial experiment is presented in [49]. Fluoroacetate dehydrogenase was soaked with photocaged fluoroacetate and pumped with 320-360 nm laser light to produce structures at 4 time points (t=0, 30, 752, and 2,052 ms). The resting state structure (0 ms) shows an empty active site, with the exception of a few water molecules, and equivalent density between the cap domains of both protein subunits. 30 ms and 752 ms after light activation a significant reduction in electron density can be observed in the cap domain of subunit B relative to subunit A. The reduction in electron density in the cap domain of subunit B coincides with the appearance of fluoroacetate in the active site of subunit A at 752 ms. The final dataset at 2,052 ms shows further structural rearrangement of the ligand, suspected to facilitate the correct geometry for S_N2 attack, and potential formation of an intermediate state in the reaction. On I24, a portable Pharos laser system which is tunable from 210-2500 nm providing femtosecond pulses can be used for light-activation. Initial experiments showed the successful activation of a photocage using 308 nm excitation with binding of the released ligand to the target protein observed. At the time of writing integration into the beamline personnel safety system is ongoing and routine user experiments are anticipated at the end of the year. For experiments when less intense pulses of light are required, light-activation with TTL controlled LEDs has been performed successfully.

FIGURE AND TABLE LEGENDS:

Figure 1: Sample loading equipment in place at Diamond Light Source. It consists of a vacuum pump (**a**), glove-box (**b**), and humidifier (**c**). Within the glove-box vacuum pressure is used to act

on a chip loaded with crystal slurry held in a sample block (**d**) attached to a Büchner flask (**e**, green arrow), via a pressure regulator (**f**, yellow arrow) attached to a stopcock (**g**, blue arrow). Humid air is pumped into the tent via plastic tubing attached to the humidifier (**h**), and measured using a hygrometer (**i**). Components are held in place using clamp stands (**j**).

Figure 2: Sample holders. They utilize a metal O-ring (**a**) to clamp polyester film onto a top (**b**) and bottom (**c**) half, with the bottom half sporting magnetic mounts (**d**) that are used to attach the sample holder to the sample stages. The polyester film (6 µm (**e**) or 3 µm (**f**)) as well as rubber O-rings (white arrows) prevent a crystal-loaded chip from drying rapidly in a sample holder which is closed tight with hex bolts (**g**). Chips are cleaned using sequential 15-minute baths in dH_2O, 1 M HCl, and dH_2O (**h**).

Figure 3: Data collection GUI for fixed target data collection at I24. (**a**) shows the main interface used for aligning chips and defining data collection parameters, (**b**) is the mapping lite interface used for defining sub-regions of a chip for data collection and (**c**) is an interface for defining parameters for laser illumination.

Figure 4: The process of mounting a chip holder onto the stages as described in Step 3, point 1.

Figure 5: Chip alignment. A chip is aligned by clicking on three fiducial markers on the chip shown in (**a**). Views of fiducials 0, 1 and 2 through the beamline on-axis viewing system are shown in (**b**), (**c**) and (**d**).

Figure 6: Auto-processing results displays launched as described in step 6.1. An updating hit-rate plot is displayed (**a**, inset). If a 'hit' is clicked on the corresponding diffraction image is displayed in dials image viewer. The hit-rate for the current data collection is shown (29.6% in this example) Panel (b) shows an example of a window showing current indexing and integration rates for data collected so far during the visit that updates in real time.

Figure 7: More in-depth data analysis. Visualization of unit cell parameters can reveal polymorphs (**a**). Average unit cell parameters are calculated; however, this does not yet extend to individual averages for polymorphs. Visualization of a small subset of data (data shown are a subset of 793 copper nitrate reductase crystals from the data described in Ebrahim *et al* 2019) is often sufficient to reveal trends. 2-D plots of useful parameters can also be produced to reveal variations that arise due to loading or dehydration effects that could be addressed for upcoming data collections (**b**). Stereographic projections can reveal the presence, or absence, preferred orientations feeding back into the loading protocol (**c**).

DISCUSSION:

Serial synchrotron data collection is a relatively new technique at MX beamlines, bridging the gap between the ultra-fast data collections currently being performed at XFELs and traditional synchrotron-based MX. This manuscript aims to give an overview of how to successfully collect fixed target serial data at beamline I24, Diamond Light Source for low dose, dose series, and time-resolved experiments. As with standard crystallography, sample preparation is a major bottle

neck in structure solution. SSX is no different, and preparation of a homogenous crystal slurry in sufficient quantities has not yet benefited from several decades of study and refinement like the growth of single large protein crystals has. However, preparation of these slurries is outside the scope of this paper and has been summarized elsewhere[50]. The critical step in the approach described here involves the careful use of the available sample using easy to use GUI interfaces (step 3) and automated data processing pipelines (step 6) to inform the chip loading (step 1) and how an experiment should proceed.

The fast feedback pipeline is a powerful tool that allows users to assess initial hit rates during data collection to inform subsequent chip loading protocols for successful data collection. When faced with a low hit rate (<5%), users risk collecting incomplete data and/or wasting beamtime with additional collections. In this case, sample could be pooled, concentrated by gentle centrifugation, and/or larger volumes could be loaded in step 1.5. A higher hit rate is generally favorable, however, there is a point of diminishing return where overloading leads to multiple crystals in the same well. DIALS is capable of dealing with multi-lattice diffraction data[51], but a greater concern than indexing and integration is the detrimental effect crystal grouping can have on the even activation of crystals by laser light or rapid mixing for precise time resolved experiments. Particular care are should therefore be taken to avoid overloading fixed targets for time resolved experiments.

The indexing and integration processing step produces a plot with the central cross representing the beam direction, each point representing the direction of the hkl 001 reflection of individual lattices, and the outer ring of the circle representing a rotation of 90° away from the beam axis. This will show if your crystals have a preferred orientation, which may impact data completeness and indicate the need to collect more data or vary the loading protocol. In the left-hand panel of **Figure 7c**, the effect of overloading a chip with HEWL crystals is shown. As apertures fill with more crystals, they stick to the angled walls of the apertures rather than wedging at the base in a random orientation. The two orthogonal ellipses are a result of crystals lying on the internal walls of the chip which are at ~35° to the beam direction. This reduces the volume of crystals loaded, reduces the hit rate, and dramatically reduces the fraction of crystals lying in these preferred planes.

It should be noted that other serial approaches are available at I24, such as LCP extruders and microfluidic chips. These use similar GUIs and the same processing pipelines so much of the above will remain applicable even if a different technique is used. A number of serial approaches exist for both SSX and SFX beyond the fixed target approach described here, each has certain advantages over the other depending on the experiment to be performed and the beamline used for the experiment. As serial approaches are evolving rapidly it is advisable to check the beamline webpages (https://www.diamond.ac.uk/Instruments/Mx/I24.html) for recent updates and talk to beamline staff at as early a stage as possible when planning beamtime. Access to I24 for standard and serial experiments is free at point of use. For UK and EU users travel and accommodation costs are partly covered through INEXT Discovery.

ACKNOWLEDGMENTS:

Enter text here.

DISCLOSURES:

Enter text here.

REFERENCES:

1. Schlichting, I., Serial femtosecond crystallography: the first five years. *IUCrJ*. **2** (2), 246-255 (2015).
2. Diederichs, K., Wang, M., Serial Synchrotron X-Ray Crystallography (SSX). In Protein Crystallography: Methods and Protocols, Wlodawer, A., Dauter, Z., Jaskolski, M., Eds. Springer New York: New York, NY, 239-272 (2017).
3. Pearson, A. R., Mehrabi, P., Serial synchrotron crystallography for time-resolved structural biology. *Current Opinion in Structural Biology*. **65**, 168-174 (2020).
4. Chapman, H. N., Structure Determination Using X-Ray Free-Electron Laser Pulses. In Protein Crystallography: Methods and Protocols, Wlodawer, A., Dauter, Z., Jaskolski, M., Eds. Springer New York: New York, NY, 295-324 (2017).
5. Chavas, L. M., Gumprecht, L., Chapman, H. N., Possibilities for serial femtosecond crystallography sample delivery at future light sources. *Structural Dynamics*. 2 (4), 041709 (2015).
6. Dauter, Z., Wlodawer, A., Progress in protein crystallography. *Protein & Peptide Letters*. **23** (3), 201-10 (2016).
7. Owen, R. L., Rudiño-Piñera, E., Garman, E. F., Experimental determination of the radiation dose limit for cryocooled protein crystals. *Proceedings of the National Academy of Sciences of the United States of America*. **103** (13), 4912-7 (2006).
8. Garman, E. F., Weik, M., X-ray radiation damage to biological samples: recent progress. *Ournal of Synchrotron Radiation*. **26** (Pt 4), 907-911 (2019).
9. Axford, D. et al. In situ macromolecular crystallography using microbeams. *Acta crystallographica. Section D, Biological crystallography*. **68** (Pt 5), 592-600 (2012).
10. Warren, A. J., Axford, D., Paterson, N. G., Owen, R. L., Exploiting Microbeams for Membrane Protein Structure Determination. *Advances in Experimental Medicine and Biology*. **922**, 105-117 (2016).
11. Sanishvili, R., Fischetti, R. F., Applications of X-Ray Micro-Beam for Data Collection. In Protein Crystallography: Methods and Protocols, Wlodawer, A., Dauter, Z., Jaskolski, M., Eds. Springer New York: New York, NY, 219-238 (2017).
12. Wierman, J. L. et al. Fixed-target serial oscillation crystallography at room temperature. *IUCrJ*. **6** (2), 305-316 (2019).
13. Maeki, M. et al. Room-temperature crystallography using a microfluidic protein crystal array device and its application to protein–ligand complex structure analysis. *Chemical Science*. **11** (34), 9072-9087 (2020).
14. Grunbein, M. L., Nass Kovacs, G., Sample delivery for serial crystallography at free-electron lasers and synchrotrons. *Acta Crystallographica Section D*. **75** (2), 178-191 (2019).
15. Weierstall, U., Liquid sample delivery techniques for serial femtosecond crystallography. *Philosophical Transactions of the Royal Society B: Biological Sciences*. **369** (1647), 20130337 (2014).
16. Botha, S. et al. Room-temperature serial crystallography at synchrotron X-ray sources

using slowly flowing free-standing high-viscosity microstreams. *Acta crystallographica. Section D, Biological crystallography*. **71** (Pt 2), 387-97 (2015).
17. Kovácsová, G. et al. Viscous hydrophilic injection matrices for serial crystallography. *IUCrJ*. **4** (Pt 4), 400-410 (2017).
18. Monteiro, D. C. F. et al. A microfluidic flow-focusing device for low sample consumption serial synchrotron crystallography experiments in liquid flow. *Journal of Synchrotron Radiation*. **26** (2), 406-412 (2019).
19. Monteiro, D. C. F. et al. 3D-MiXD: 3D-printed X-ray-compatible microfluidic devices for rapid, low-consumption serial synchrotron crystallography data collection in flow. *IUCrJ*. **7** (Pt 2), 207-219 (2020).
20. Mueller, C. et al. Fixed target matrix for femtosecond time-resolved and in situ serial micro-crystallography. *Structural Dynamics*. **2** (5), 054302 (2015).
21. Owen, R. L. et al. Low-dose fixed-target serial synchrotron crystallography. *Acta Crystallographica Section D: Structural Biology*. **73** (Pt 4), 373-378 (2017).
22. Keedy, D. A. et al. Mapping the conformational landscape of a dynamic enzyme by multitemperature and XFEL crystallography. *Elife*. **4** (2015).
23. de la Mora, E. et al. Radiation damage and dose limits in serial synchrotron crystallography at cryo- and room temperatures. *Proceedings of the National Academy of Sciences*. **117** (8), 4142-4151 (2020).
24. Barends, T. R. et al. Direct observation of ultrafast collective motions in CO myoglobin upon ligand dissociation. *Science*. **350** (6259), 445-50 (2015).
25. Pande, K. et al. Femtosecond structural dynamics drives the trans/cis isomerization in photoactive yellow protein. *Science*. **352** (6286), 725-9 (2016).
26. Standfuss, J., Spence, J., Serial crystallography at synchrotrons and X-ray lasers. *IUCrJ*. **4** (2), 100-101 (2017).
27. Grünbein, M. L. et al. Illumination guidelines for ultrafast pump–probe experiments by serial femtosecond crystallography. *Nature Methods*. **17** (7), 681-684 (2020).
28. Mehrabi, P. et al. Liquid application method for time-resolved analyses by serial synchrotron crystallography. *Nature Methods*. **16** (10), 979-982 (2019).
29. Beyerlein, K. R. et al. Mix-and-diffuse serial synchrotron crystallography. *IUCrJ*. **4** (Pt 6), 769-777 (2017).
30. Schmidt, M., Mix and Inject: Reaction Initiation by Diffusion for Time-Resolved Macromolecular Crystallography. *Advances in Condensed Matter Physics*. 2013, 167276 (2013).
31. Kupitz, C. et al. Structural enzymology using X-ray free electron lasers. *Structural Dynamics*. **4** (4), 044003 (2017).
32. Stagno, J. R. et al. Structures of riboswitch RNA reaction states by mix-and-inject XFEL serial crystallography. *Nature*. **541** (7636), 242-246 (2017).
33. Shilova, A. et al. Current status and future opportunities for serial crystallography at MAX IV Laboratory. *Journal of Synchrotron Radiation*. **27** (5), 1095-1102 (2020).
34. Huang, C.-Y. et al. In meso in situ serial X-ray crystallography of soluble and membrane proteins. *Acta Crystallographica Section D*. **71** (6), 1238-1256 (2015).
35. Gao, Y. et al. High-speed raster-scanning synchrotron serial microcrystallography with a high-precision piezo-scanner. *Journal of Synchrotron Radiation*. **25** (5), 1362-1370 (2018).
36. Beale, J. H. et al. Successful sample preparation for serial crystallography experiments.

Journal of Applied Crystallography. **52** (Pt 6), 1385-1396 (2019).
37. Doak, R. B. et al. Crystallography on a chip - without the chip: sheet-on-sheet sandwich. *Acta Crystallographica Section D: Structural Biology*. **74** (Pt 10), 1000-1007 (2018).
38. Axford, D., Aller, P., Sanchez-Weatherby, J., Sandy, J., Applications of thin-film sandwich crystallization platforms. *Acta Crystallographica Section F: Structural Biology Communications*. **72** (Pt 4), 313-9 (2016).
39. Davy, B. et al. Reducing sample consumption for serial crystallography using acoustic drop ejection. Journal of Synchrotron Radiation. **26** (5), 1820-1825 (2019).
40. Brewster, A. S. et al. Improving signal strength in serial crystallography with DIALS geometry refinement. *Acta Crystallographica Section D*. **74** (9), 877-894 (2018).
41. Winter, G. et al. DIALS: implementation and evaluation of a new integration package. *Acta Crystallographica Section D*. **74** (2), 85-97 (2018).
42. Ebrahim, A. et al. Resolving polymorphs and radiation-driven effects in microcrystals using fixed-target serial synchrotron crystallography. *Acta Crystallographica Section D*. **75** (2), 151-159 (2019).
43. Brehm, W., Diederichs, K., Breaking the indexing ambiguity in serial crystallography. *Acta Crystallographica Section D*. **70** (1), 101-109 (2014).
44. White, T., Processing serial crystallography data with CrystFEL: a step-by-step guide. *Acta Crystallographica Section D*. **75** (2), 219-233 (2019).
45. Shi, Y., Liu, H., EM-detwin: A Program for Resolving Indexing Ambiguity in Serial Crystallography Using the Expectation-Maximization Algorithm. *Crystals*. **10** (7), 588 (2020).
46. Gildea, R. J., Winter, G., Determination of Patterson group symmetry from sparse multi-crystal data sets in the presence of an indexing ambiguity. *Acta Crystallographica Section D*. **74** (5), 405-410 (2018).
47. Ebrahim, A. et al. Dose-resolved serial synchrotron and XFEL structures of radiation-sensitive metalloproteins. *IUCrJ*. **6** (4), 543-551 (2019).
48. Rabe, P. et al. Anaerobic fixed-target serial crystallography. *IUCrJ*. **7** (5), 901-912 (2020).
49. Schulz, E. C. et al. The hit-and-return system enables efficient time-resolved serial synchrotron crystallography. *Nature Methods*. **15** (11), 901-904 (2018).
50. Beale, J. H. et al. Successful sample preparation for serial crystallography experiments. *Journal of Applied Crystallography*. **52** (6), 1385-1396 (2019).
51. Gildea, R. J. et al. New methods for indexing multi-lattice diffraction data. *Acta Crystallographica Section D*. **70** (10), 2652-2666 (2014).

Figure

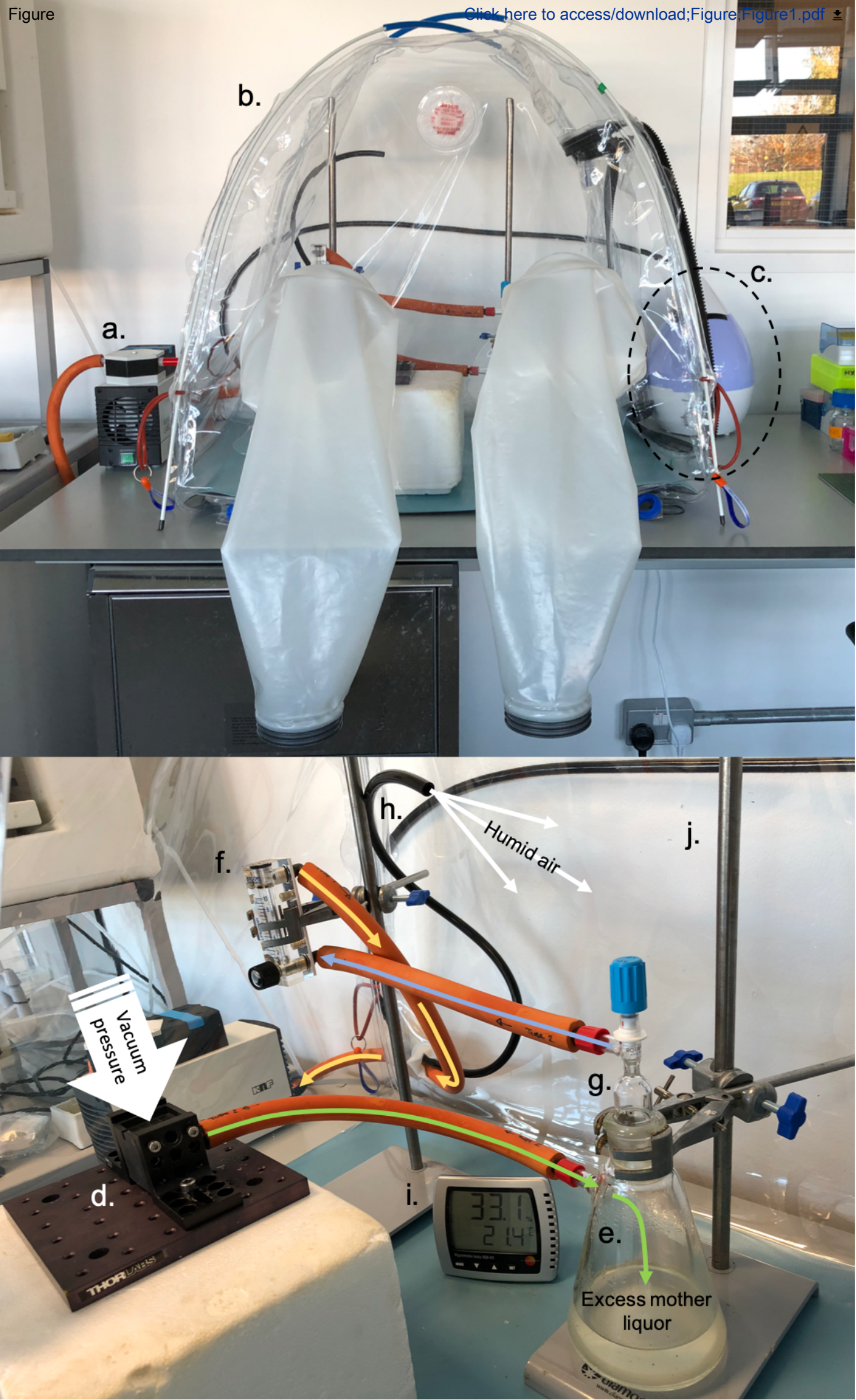

Figure

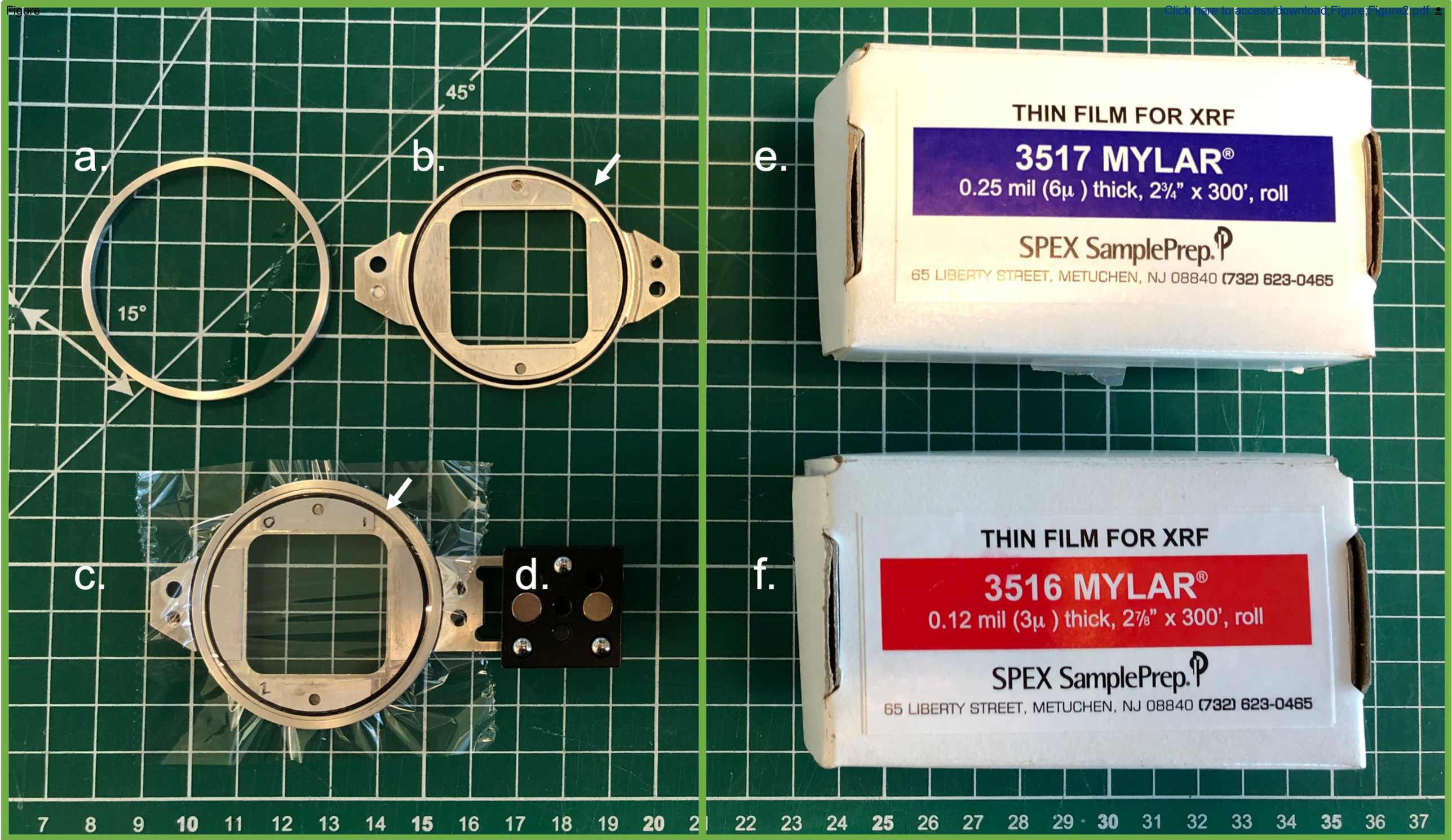

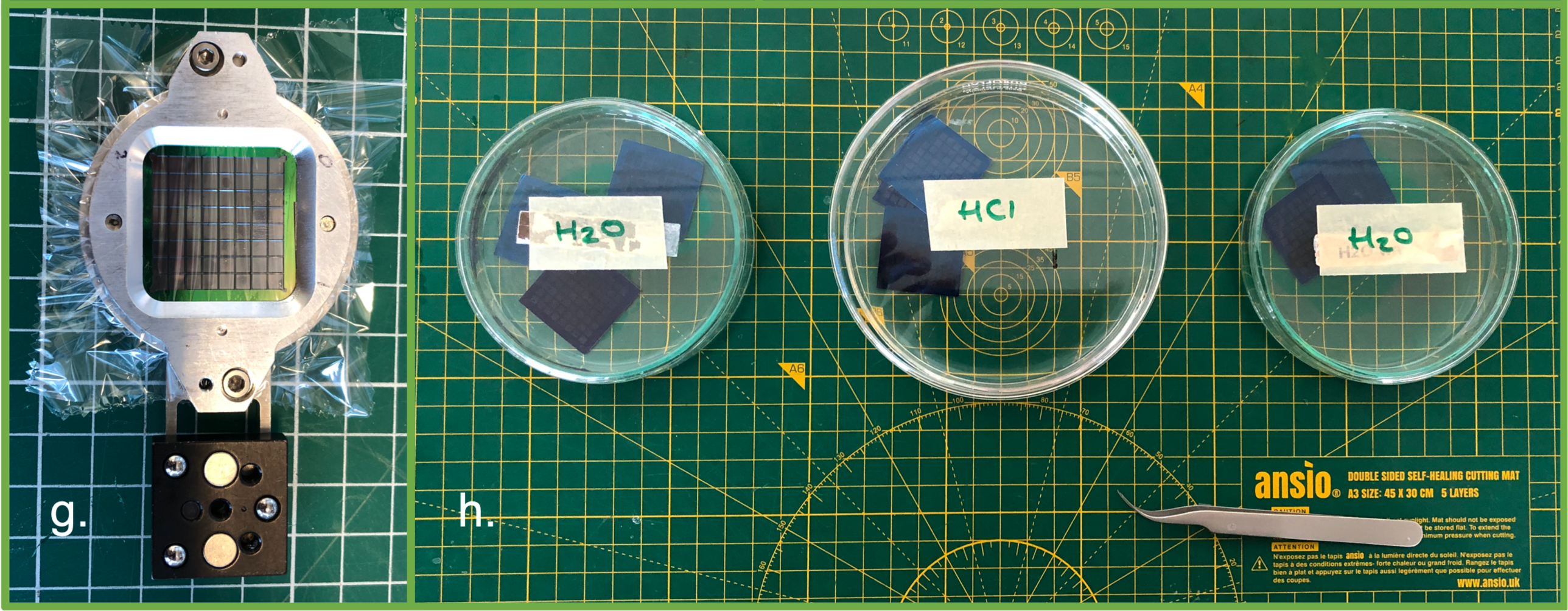

Figure

Click here to access/download;Figure;Figur

a

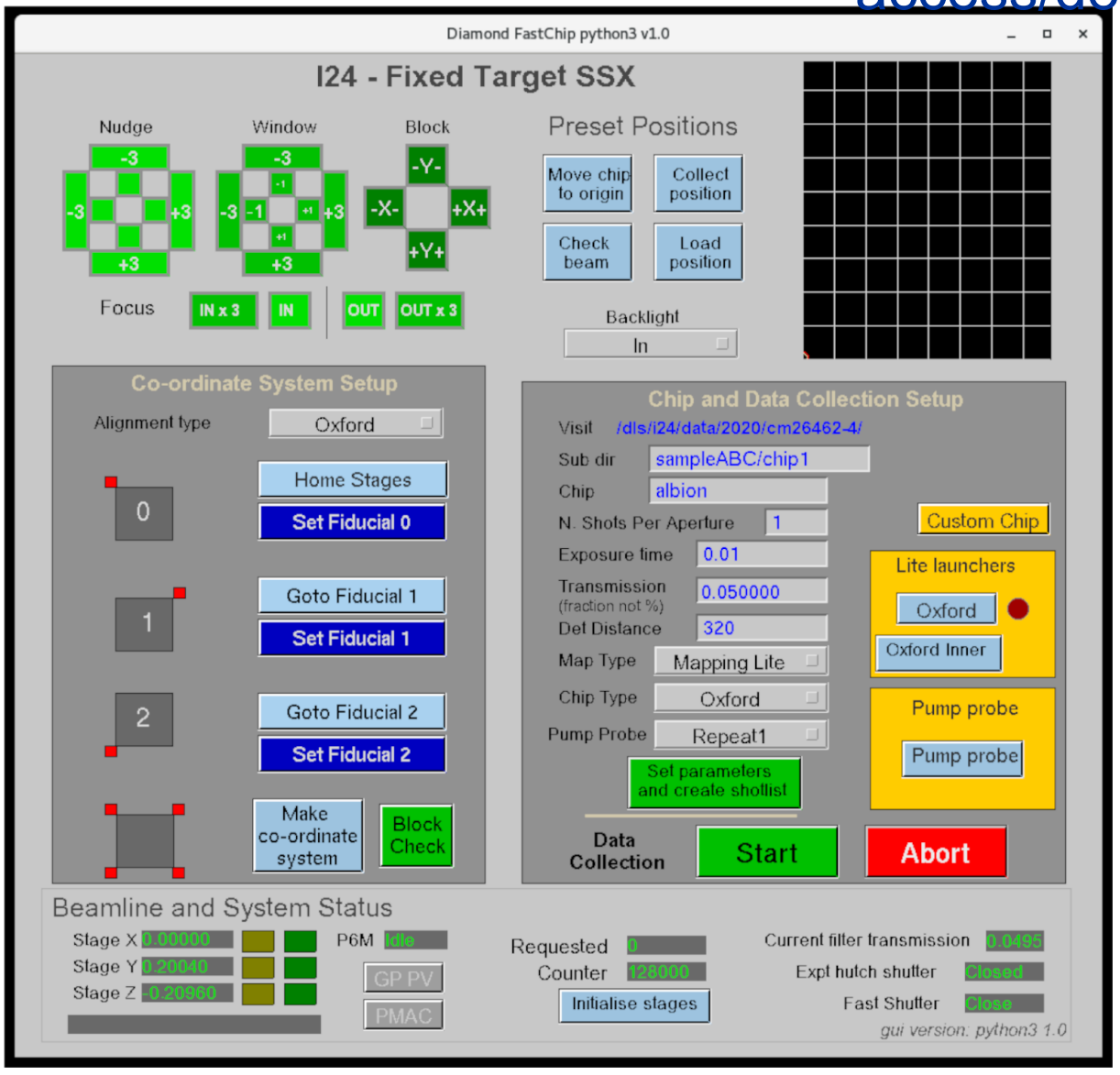

b

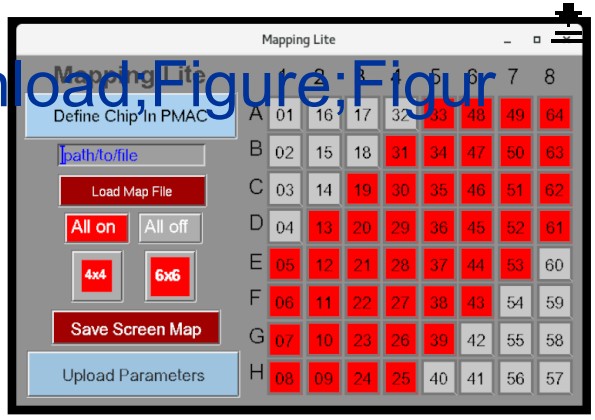

c

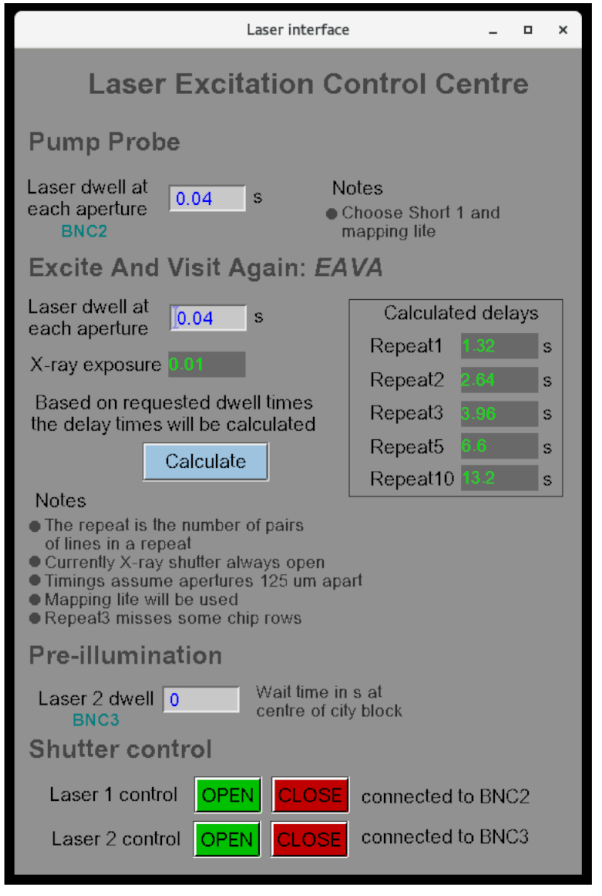

Figure4

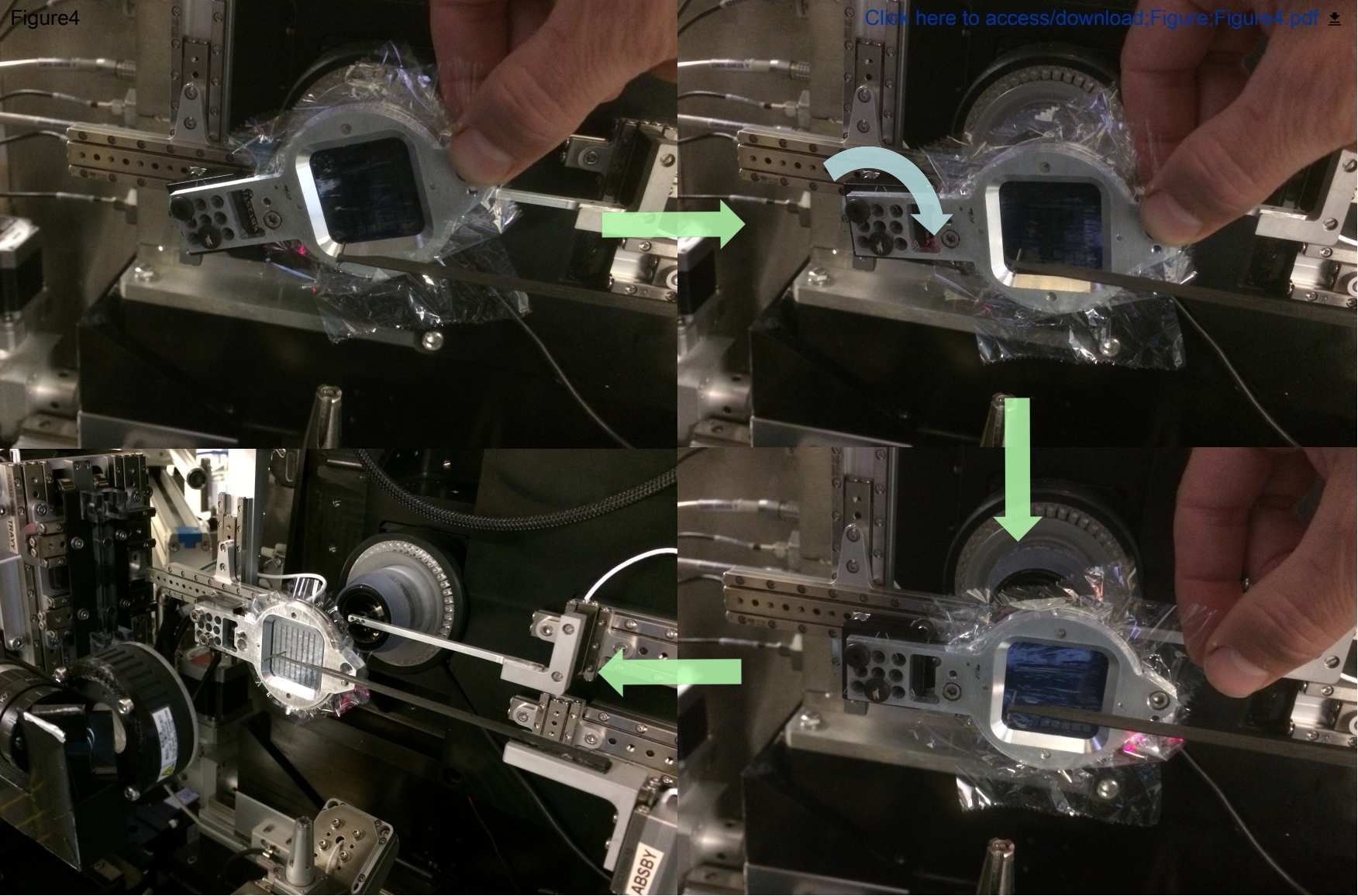

Figure

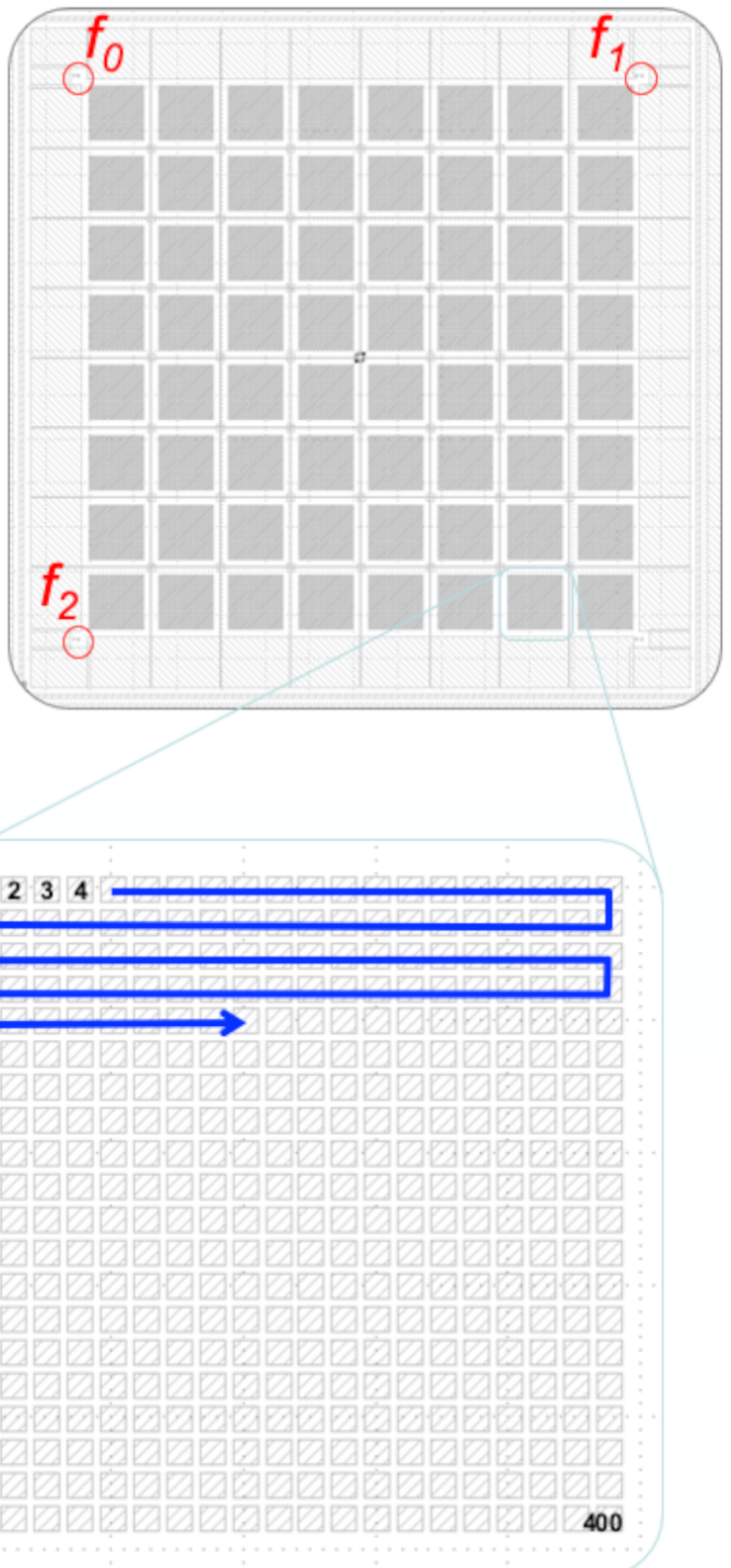

Figure

a

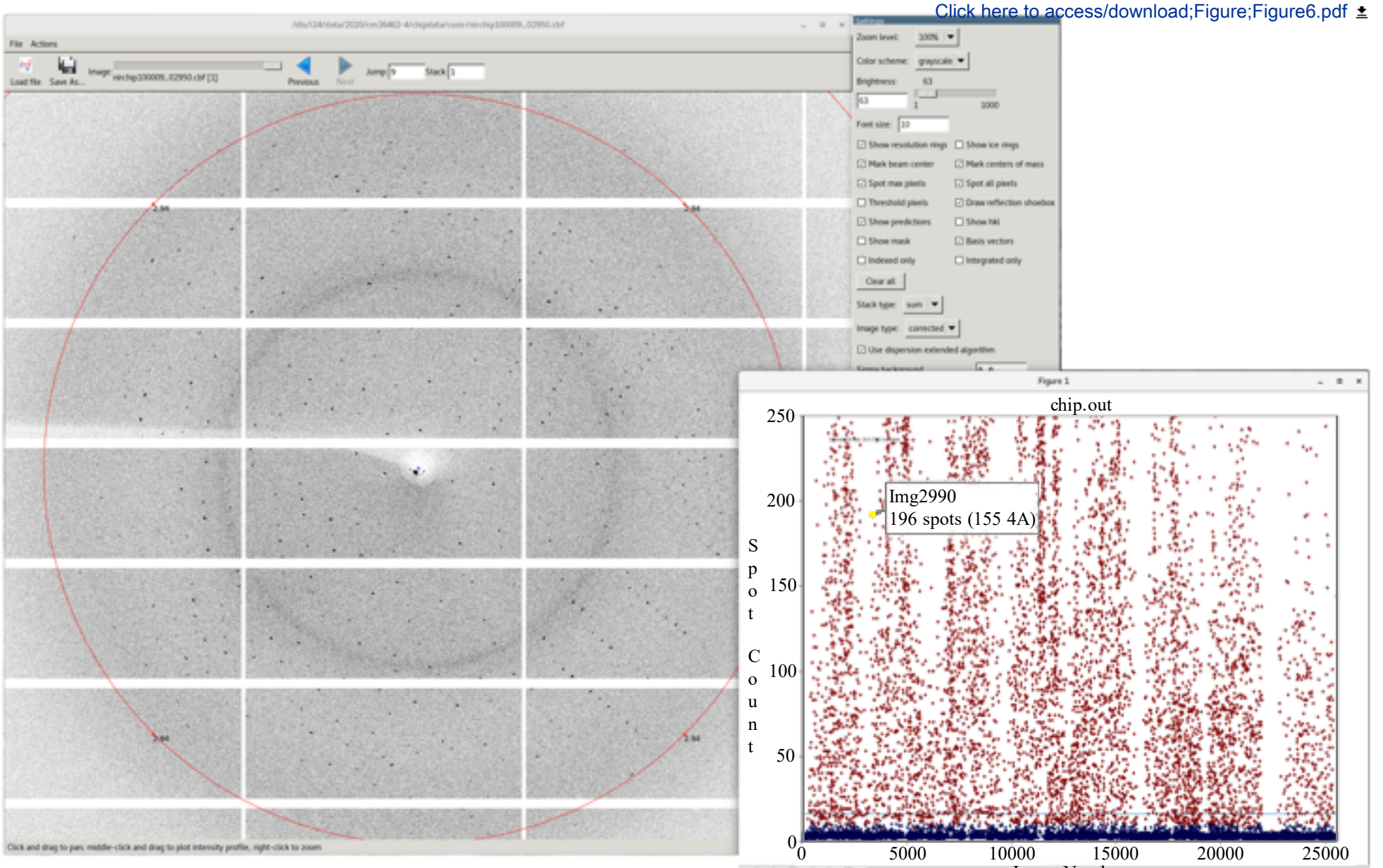

b

Name	Processed	Indexed	%	Integrated	%	
atomic	25600	10737	16%	14025	55%	
busted_JR	25600	11009	43%	14698	57%	
cheeky	3500	1520	43%	2628	75%	
dakota_JR	25600	6049	24%	7710	30%	
europe_JR	22200	958	4%	1040	5%	
fergie_JR	25600	10142	40%	13247	52%	
goldie_JR	25600	9153	36%	11639	45%	
hardfi_JR	25600	7494	29%	9166	36%	
jarule	25600	9418	37%	12398	48%	
mansun	25600	10211	40%	15908	62%	
mansun_JR	25600	10692	42%	17943	70%	
nolans	25600	7470	29%	11097	43%	
nolans_JR	25600	7689	30%	11932	47%	
others	25600	5000	20%	6978	27%	
pogues	5480	2445	45%	3539	65%	\
quincy	8636	4155	48%	5715	66%	|
rascal	7351	4127	56%	5845	80%	/
smiths	801	268	33%	359	45%	-
travis	16315	10061	62%	14771	91%	\

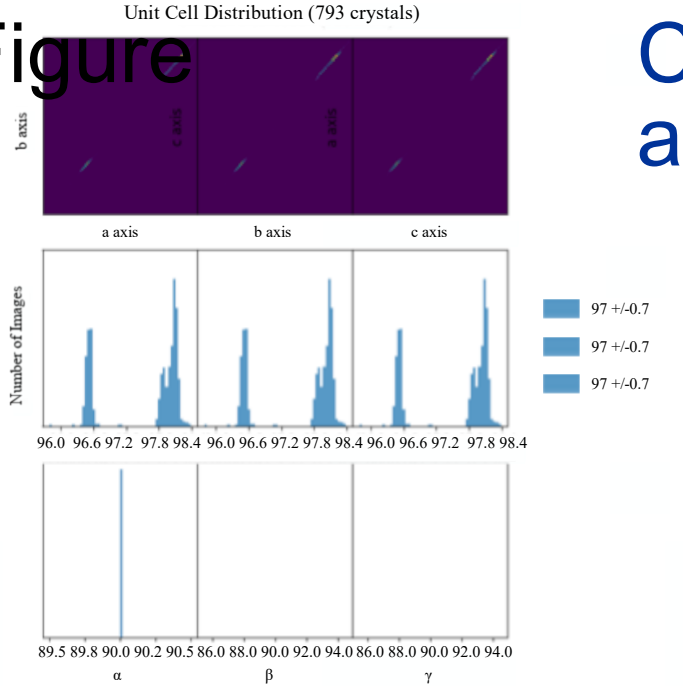

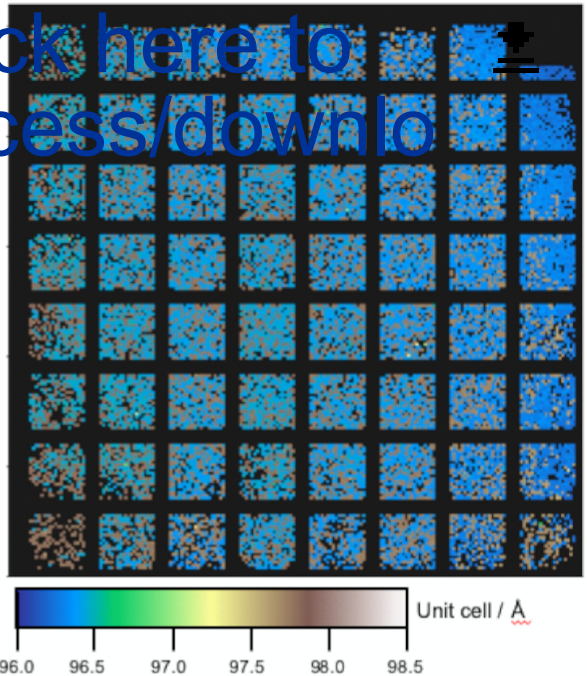

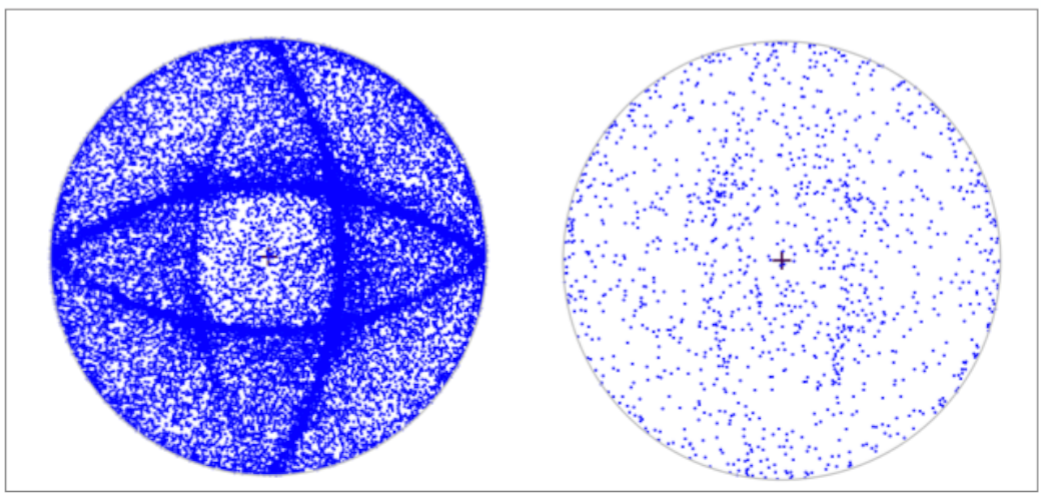

Table of Materials

Click here to access/download;Table of Materials;JoVE_Table_of_Materials.xlsx

Name of Material/Equipment	Company	Catalog Number
Chip Holders	Custom Built	N/A
Chipless Chip Spacers	SWISCII	N/A
Geobrick LV-IMS-II	Delta Tau	N/A
Kinematic Mounts	ThorLabs	KB25/M
KNF Laboport Vacuum Pump	Merck	Z262285-1EA
Mylar Sheets 6 µm	Fisher Scientific	15360562
Mylar Sheets 3 µm	Fisher Scientific	04-675-4
Pelco easiGlow Glow Discharge System	Ted Pella, INC.	91000
Silicon Chips	University of Southampton	N/A
Translation Stages	Smaract	N/A
1byOne Humidifier (701UK-0003)	1byOne	B01DENO0EQ

Comments/Description

In-house custom built metallic chip holders consisting of 2 magnetic base plates, 2 metal rings, and a kinematic mount.
LCP adhesive sheets available as part of the LCP modular range
A multi-axis controller/amplifier with a custom Diamond Light Source hardware configuration
Square bases with 3 magnets arranged in a triangle affixed to chip holders.

Solid PTFE vauum pump, 10 l/min pumping speed.
300 ft roll of 6 µm thick mylar XRF film by SPEX SamplePrep
300 ft roll of 3 µm thick mylar XRF film by SPEX SamplePrep

A compact stand alone glow discharge system used to produce hydrophillic surfaces

Custom etched silicon chips with 25,6000 apertures available in a variety of sizes.
XYZ sample stages are a collaborative design by Diamond Light Source and SmarAct, custom-built by SmarAct using three linear translation 50mm travel stages, precise crossed roller guideways, and an integrated sensor with up to 1 nm resolution

Commercially available 1.3 Litre ultrasonic humidifier

jove JOURNAL OF VISUALIZED EXPERIMENTS
1 Alewife Center #200
Cambridge, MA 02140
tel. 617.945.9051
www.jove.com

Standard Manuscript Template

Please Remove all Gray Text before Submitting

This template contains the sections and formatting for a submission to *JoVE*. Please begin writing directly in this document and remove the header, the footer, links, and any gray text prior to submission.

TITLE: (Instructions)

Fixed target serial data collection at Diamond Light Source

AUTHORS AND AFFILIATIONS: (Instructions)

Sam Horrell[1], Danny Axford[1], Nicholas E. Devenish[1], Ali Ebrahim[1,2], Michael A. Hough[2], Darren A. Sherrell[1], Selina L. S. Storm[1], Ivo Tews[3], Jonathan. A. R. Worrall[2], Robin L. Owen[1]*

1. Diamond Light Source, Harwell Science and Innovation Campus, Didcot, Oxfordshire OX11 0DE, UK
2. School of Biological Sciences, University of Essex, Wivenhoe Park, Colchester CO4 3SQ, UK,
3. Biological Sciences, Institute for Life Sciences, University of Southampton, Highfield Campus, Southampton SO17 1BJ, United Kingdom

KEYWORDS: (Instructions)

Serial Crystallography, Structural Biology, Macromolecular crystallography,

SUMMARY: (Instructions)

A comprehensive guide to fixed target sample preparation, data collection, and data processing for serial synchrotron crystallography at Diamond beamline I24.

ABSTRACT: (Instructions)

Serial data collection is a relatively new technique for synchrotron users. A user manual for fixed target data collection at I24, Diamond Light Source is presented with detailed step-by-step instructions, figures, and videos for smooth data collection.

INTRODUCTION: (Instructions)

Serial synchrotron crystallography (SSX) is an emerging method of data collection which was inspired by X-ray free electron lasers (XFEL) [1-3]. At an XFEL, a single diffraction pattern is recorded from a, usually very small, protein crystal before the crystal is destroyed by the extremely bright X-ray pulse. This means, typically, that a new crystal must be introduced into the X-ray beam to obtain another diffraction pattern [4]. This need to continually replenish crystals has driven the development of many serial sample delivery techniques [5].

At synchrotrons, classic (non-serial) rotation crystallography methods are widely applied, exploiting a single large crystal which is rotated in an X-ray beam using a goniometer to collect a complete dataset for structure solution [6]. In order to increase the lifetime of crystals so that a complete dataset can be collected [7] [8], and also to facilitate shipping and automated sample transfer, crystals are cryocooled to ~100 K for data collection. At intense microfocus beamlines, multi-crystal strategies are frequently employed as radiation damage can prohibit the collection of a complete dataset from a single crystal [9-11]. Despite the limits imposed by radiation damage,

the number of crystals used remains relatively modest and the approach used is essentially identical to the single crystal experiment.

SSX, on the other hand, uses serial sample delivery to obtain single still diffraction patterns from thousands of randomly orientated crystals to generate a complete dataset. ~~We~~ It is noted that serial techniques incorporating crystal rotation are under development [12-13] though here focus on still, zero rotation, approaches. There are a wide variety of sample delivery systems with different advantages and disadvantages [14], ranging from delivering a stream of crystals in a flow focused/viscous jet [15-17], microfluidic chip [18-19], or crystals on a fixed target such as an etched silicon chip [20-21]. Typically, crystals are held at room temperature, allowing greater conformational diversity to be observed and providing a more physiologically relevant environment [22]. SSX enables the collection of very low dose datasets [23], as the total dose of the dataset is equivalent to a single short X-ray exposure of one crystal. Another major advantage SSX provides is the study protein dynamics through time-resolved methods, with reactions triggered by exposure to laser light [24-27] or by mixing of crystals and ligand/substrate [28-29]. Using smaller crystals means laser light can penetrate the entirety of the crystal, uniformly initiating the reaction without multiphoton absorption to provide well defined reaction intermediates for diffraction data taken at different time points [27]. Use of larger crystals and rotation-based data collection methods suffers from a limited laser penetration depth, nonuniform or multiphoton activation, radiation damage, and mechanical overhead time within data sweeps, resulting in a mix of reaction intermediates which can prove difficult or impossible to interpret at faster reaction speeds. Smaller crystals provide a similar advantage in mixing experiments, as ligands can rapidly and more uniformly diffuse throughout the crystal, again allowing defined reaction intermediates to be recorded at different time delays [30-32].

At Diamond's microfocus beamline I24 both conventional rotation and SSX experiments can be performed. Here ~~we present~~ a comprehensive protocol for SSX sample preparation and data collection using fixed targets at I24 and protocols for data analysis of serial data at Diamond are presented. While the manuscript and accompanying videos should allow users to carry out a successful SSX experiment at I24, it should be noted that this is a rapidly developing field and approaches are continually evolving. It should also be noted that serial methods are available at other synchrotron sources, including but not limited to Petra III (P14-TREXX), MAX IV (BioMAX) [33], SLS (PXI and PXII) [34], and NSLS (FMX) [35], and that the specifics of serial data collection and processing will differ but the core principles will remain the same. The protocols below should be seen to represent a starting point and a pathway to base camp rather than the summit of what might be achieved.

PROTOCOL: (Instructions)

This protocol assumes the users~~you~~ have a protein or small molecule crystal system, from which ~~you have been able to produce~~ a microcrystal slurry on the order of 0.5-2.0 ml with a good density of microcrystals per ml has been produced. Protocols for obtaining crystal slurries are described in [36]. Many different types of fixed target are available, the most commonly used at I24 utilise a precisely defined silicon chip. In order to differentiate from other chip layouts, below and in the beamline interface this is referred to as an 'Oxford chip'. As previously described the Oxford chip

layout comprises 8×8 'city blocks', each containing 20×20 apertures for a total of 25,600 apertures [20-21].

1. Preparing and Loading a Chip

The process occurs within a humidity-controlled environment (Figure 1), typically 80% or higher relative humidity, to prevent protein crystals from drying out. Once loaded and sealed, crystals can survive for upwards of 24 hours. However, this is can vary greatly between crystal systems. Within the chamber ~~you will require~~ a low powered vacuum pump attached to a loading stage to hold a silicon chip (Figure 1), a silicon chip, a chip holder with ~~mylar~~ polyester foil (~~see below~~Figure 2), a p200 pipette, 200 µl pipette tips, tweezers, filter paper and your protein crystal slurry are required .

1.1 Prepare a chip holder

1.1.1 Cut two sheets of ~~mylar~~ polyester foil into squares approximately 6×6 cm.

1.1.2 Lay the ~~mylar~~ polyester sheets over the two base plates (large and small).

1.1.3 Fix the ~~mylar~~ polyester sheets in place using the metal sealing rings.

1.1.4 Carefully pull on the excess ~~mylar~~ polyester foil to remove any creases to make visualizing and centering samples easier later.

1.2 Select a silicon chip with appropriately sized apertures (7-30 µm) relative to the size of your crystals.

~~1.3~~ Glow discharge your chip for 25 seconds at 0.39 mBar and using a current of 15 mA

~~1.4~~1.3 to enable easy spreading of micro crystals on the chip.

~~1.5~~1.4 Place the silicon chip on the chip loading stage using tweezers with the raised bars facing down.

~~1.6~~1.5 Apply 200 µL~~l~~ of your micro-crystal slurry to the flat side of the chip using a pipette.

~~1.7~~1.6 Spread out your crystal slurry to cover all the "city-blocks" of the chip.

1.7 If your chip is damaged, cover any holes with a small piece of polyester foil~~mylar~~ or filter pipette tip to ensure an even vacuum can be applied.

1.8 Apply a gentle vacuum until all excess liquid has been sucked through the chip.

1.9 Remove the chip from the chip loading stage with tweezers.

1.10 Carefully blot the underside of the chip with filter paper to remove excess liquid.

1.11 Place the loaded chip on the larger half of the chip holder between the guide marks flat side down.

Formatted: Not Highlight
Formatted: Not Highlight
Formatted: Not Highlight
Formatted: Not Highlight
Formatted: Not Highlight
Formatted: Line spacing: 1.5 lines
Formatted: Font color: Text 1
Formatted: Font color: Text 1
Formatted: Line spacing: 1.5 lines

1.12 Seal the chip by placing the small half of the chip holder on top.

1.12.1 The two halves of the chip holder will~~should~~ snap into place, if the second half does not sit flush spin the holder 180° to properly align the magnets.

1.13 Screw the chip holder closed with hex bolts to fix the chip securely in place.

Alternatively, a "chipless" chip can be loaded in a similar fashion, with a smaller volume of crystal slurry (~15 µl) sandwiched between the two layers of ~~mylar~~ polyester foil in the chip holder [37], or a smaller volume can be loaded using a 50 µm thick double-sided adhesive spacer applied directly to the ~~mylar~~ polyester foil~~film~~ as described in [38]. The use of adhesive spacers also allows multiple samples (or variants of samples such as ligand soaks) to be loaded on each chipless chip. A complementary loading approach exploiting acoustic drop ejection (ADE) to load silicon chips can also be used at Diamond [39]. ADE allows chips to be loaded using smaller volumes of crystal slurry than pipette loading. It is a particularly useful technique when samples are scarce, though the chemical composition and viscosity of the slurry must be taken into consideration.

Formatted: Not Highlight

2 GUI and Setup at The Beamline

All chip alignment and setup for data collection is done through a simple EPICS Display Manager (edm) graphical user interface (GUI) (figure 3a). This provides a point and click interface to beamline instrumentation and provides input parameters for python-based data collection. Sub windows provide additional control for collecting from sub regions of a sample holder (figure 3b) or laser/LED pump-probe experiments (figure 3c).

3 Aligning the Chip

Formatted: Line spacing: 1.5 lines

3.1 Place the loaded chip on the XYZ stage at the beamline (shown in figure 4a) using the kinematic mounts.

3.1.1 Take care to avoid pulling the stages along their direction of travel. The magnets in the kinematic mounts are quite strong so this can be done quite easily by accident.

3.1.2 When approaching the mount, the chip holder should be held at a slight angle (+/-30°) ~~so it is pointing slightly up towards ~2pm or down towards ~4pm~~. When the magnets make contact allow the chip holder to rotate ~~to 3pm~~ parallel to the floow (0°) and the chip holder will click into place (figure 4b).

3.1.3 When unloading a chip follow a reverse path. Rotate and angle the chip away from the stages before pulling the chip holder away.

3.2 Using the beamline's on-axis viewing system and the chip alignment GUI, locate the top left fiducial of the chip

3.3 Fiducials are three squares, two small and one large, at right angles to one another (figure 5a).

3.4 The chip is back illuminated so the chip will appear dark with apertures as white squares.

3.5 Centre on fiducial zero in X, Y, and Z (figure 5b).

3.6 X and Y are aligned by moving left/right and up/down, respectively.

3.7 Z is aligned by moving the chip in and out of focus.

3.8 Click "set fiducial zero".

3.9 Repeat steps 2-4 for fiducial one (top right, figure 5c) and fiducial two (bottom left, figure 5d) to align all fiducials with the X-ray beam.

3.10 Generate a co-ordinate matrix by pressing 'make co-ordinate system', this calculates the offset, pitch, roll, and yaw of the chip relative to the stages allowing all subsequent movements to be done in the chip co-ordinate frame.

3.11 Click "block check" to move the XYZ stage to the first well of each city block for visual confirmation that the chip is well aligned.

3.12 If the X-ray crosshair lines up with the apertures the chip is aligned. If not, repeat steps 2-7.

NOTES: In case of difficulty aligning (broken fiducials), different apertures on the chip can be used for alignment using the "alignment type" pull-down menu. ~~A new python GUI, offering move-on-click functionality and automated chip alignment is currently under development, but is not yet ready for routine use at the time of the writing of this manuscript.~~

Many different types of chip are available for fixed target data collection. Different chip types are accommodated through use of the 'chip type' pull-down menu. The most common chip types used at I24 are '~~o~~Oxford' and 'custom' chips. The number and the spacing of apertures and fiducials on the chip are read from a chip dictionary defined *via* the pull-down menu. Custom chip allows the aperture spacing to be defined on-the-fly, which is particularly useful for thin-film sheet-on-sheet or other 'chipless' type chips where crystals are randomly located across the holder [37]. A new python GUI, offering move-on-click functionality and automated chip alignment is currently under development, but is not yet ready for routine use at the time of the writing of this manuscript.

4 Setting up Data Collection

Formatted: Not Highlight

Formatted: Not Highlight

Formatted: Line spacing: Multiple 1.15 li

Data collection setup will depend on the system ~~you are studying~~being studied, and the experiment ~~you wish~~ to be performed. This can range from the simplest SSX experiment, collecting a low dose structure, to a time-resolved experiment using lasers or rapid mixing to initiate a reaction which will require multiple complete datasets at different time delays. To set up a data collection the following parameters need to be defined.

4.1 *Experimental variables*: Folder, filename, exposure time, transmission, detector distance, and number of shots per aperture should be filled in as appropriate.

4.2 *Chip type*: As described above, chip type should match the chip in use.

4.2.1 If a thin film or 'chipless' chip is being used, then the chip type should be set to '*none*'.

4.2.2 The number of steps and step size in both *x* and *y* are defined in the GUI.

4.3 *Map type*: this allows subsections of a chip to be selected for data collection (*see figure 3b)*.

4.3.1 '*None*' means data are collected from every aperture on a chip.

4.3.2 '*Lite*' means data are collected from selected city blocks on the chip (*see figure 3b*).

4.3.2.1 This can be useful if, for example, a region of a chip is known to be poorly loaded or empty.

4.4 '*Full*' allows individual apertures to be selected for data collection.

4.4.1 In this case a correctly formatted text file must be provided.

4.5 *Pump-probe*: Select the type of pump probe experiment and the desired time delay. The triggering of the pump (usually a LED or laser) is often specific to a particular experiment, so will not be described in detail here.

4.5.1 'Short' delays refer to experiments when there is a dwell at each aperture between the pump and the probe. i.e. pump, probe, move to the next sample. Delays are typically ~~of~~ on the order of 1 second~~s~~ or tens~~10s~~ of milliseconds.

4.5.2 'Long' delays refer to an excite and visit again (EAVA) strategy, where apertures are visited twice, with a defined time delay between visits, i.e. pump, move, pump, move, probe, move, probe, etc. The time delay is calculated based on the requested laser and X-ray exposure times (figure 3c) and is typically ~1 second~~s~~ or more.

5 Common Data Collection Methods

Formatted: Line spacing: 1.5 lines

Formatted: Not Highlight

The following are the key parameters that define the type of experiment ~~you are~~being ~~carryi~~carried~~ng~~ out. This section assumes that ~~you have filled out~~ the other settings from protocol 3 "Setting up Data Collection" have been defined.

5.1 Scenario 1: Low-dose data collection. Collection of a single diffraction image from every selected aperture on the sample holder.

5.1.1 Set number of shots per aperture to 1.

5.1.2 Set pump probe to 'none'.

5.2 Scenario 2: A dose series, collecting *n* images sequentially from every selected aperture on the sample holder. The chip is stationary at each aperture while each set of *n* images is collected.

5.2.1 Set the number of shots per aperture to '*n*'. Note that processing is simplified if *n*=5, 10, 20 or another multiple of 10. ~~In our experience i~~It is difficult to establish trends if n < 5. It is useful to consider the total time required to cover a chip and the number of image files produced when *n* is increased.

5.2.2 Set pump probe to 'none'.

5.3 **Scenario 3**: Pump-probe methods

5.3.1 Select a method from the "pump probe" pull-down menu to open the Laser Excitation Control Centre.

5.3.2 For a pump probe experiment fill in the 'Laser Dwell at each aperture' option.

5.3.3 For EAVA fill in the 'Laser Dwell at each aperture' and 'X-ray exposure' and click calculate.

5.3.4 Select the appropriate 'Repeat' option in the edm GUI pump probe drop-down menu for the desired delay time.

5.3.5 If your experiment requires a pre-illumination step ~~just~~ fill in the 'Laser 2 Dwell' section.

After all experimental variables are defined press 'Set parameters and create short list'. This loads experimental variables onto the geobrick controller. After this is done pressing 'Start' will move the detector in, the backlight out, and start data collection. At all points in setting up data collection it is useful to have a terminal window open where feedback on the status and outcome of each of the steps is printed.

6 Data Processing

Broadly speaking data processing can be divided into three groups based on the urgency with which feedback is required. (1) Fast feedback is required to show if crystals are present and diffract, and if so, in what numbers. This should keep up with data collection. (2) Performing data indexing and integration which can be slower but should still be performed on comparable time scales with data collection. (3) Merging and scaling of reflection intensities into an mtz file for structure solution and the generation of electron density maps represents the final step and can be slower still. Here ~~we will discuss~~ starting pipelines at I24 for the first two stages only will be discussed, as they are required for real-time feedback to guide your experiment, though note that metrics such as hit-rates and scaling statistics are not a substitute for inspecting electron density.

which may provide the only confirmation that a ligand has bound, or a reaction occurred, *in crystallo*.

6.1 Fast Feedback

6.1.1 To load the data processing modules type 'module load i24-ssx' into the terminal on any beamline workstation.

6.1.2 To run the hit-finding analysis type 'i24-ssx /path/to/visit/directory/' into the terminal. *e.g*. 'i24-ssx /dls/i24/data/2020/mx12345-6/'

6.1.2.1 This opens three terminal windows and, once data has been written to disk, a graphical representation of spot finding results from Diffraction Integrations for Advanced Light Sources (DIALS) [40-41] (Figure 6a).

6.1.2.1.1 Default settings scores every 10th image and refreshes every few seconds to minimise the computational load.

6.1.2.1.2 The default can be changed by adding an argument to the end of the command above. For example, 'i24-ssx /dls/i24/data/2020/mx12345-6 2' i24-ssx would run hit finding on every other image. However, this can put undue strain on the cluster (a shared resource!) and slow down processing times.

6.1.2.1.3 The graph is colour coded based on the likelihood of successful indexing, red shows at least 15 Bragg spots have been found (good chance of indexing), blue shows little to no useful diffraction.

6.1.2.1.4 Diffraction images of interest can be viewed in the DIALS image viewer by clicking on the spots on the spot finder interface.

6.2 Indexing and Integration Feedback

Indexing and integration of diffraction data are performed with DIALS using the dials.still_process function [40-41]. As such, specific information relating to your crystal (expected crystal space group, unit cell, and an experiment geometry) should be put into a .phil text file.

6.2.1 Load DIALS modules by typing 'module load dials' in a terminal.

6.2.2 To begin processing a dataset type 'dials.still_process /path/to/images/ /pathto/phil-file.phil'

6.2.2.1 The progress of all still processing datasets can be monitored by running the 'stills_monitor' script by typing monitor_stills_process.py (after performing module load i24-ssx and changing directory to the current visit) (Figure 6b)

6.2.3 The unit cell distribution of indexed diffraction data (Figure 7a) can be monitored using the command 'ctbx.xfel.plot_uc_cloud_from_experiments/path/to/dials/output/*refined.expt combine_all_input=true' This is particularly useful to identify and resolve unit cell polymorphs as seen in [42].

6.2.4 If, and how, this distribution varies across a fixed target can be visualised by producing a 2D plot (figure 7b) using the command 'python pacman.py /visit/processing/_hit_finding/chip.out'

Formatted: Font: (Default) +Body (Calibri)

Formatted: Font: (Default) +Body (Calibri)

Formatted: Font: (Default) +Body (Calibri)

Formatted: Font: (Default) +Body (Calibri)

Formatted: Font: (Default) +Body (Calibri)

Formatted: Font: (Default) +Body (Calibri)

Formatted: Font: (Default) +Body (Calibri)

6.2.5 Stereographic projections of all indexed diffraction data (figure 7c) are also informative. These can be produced using the DIALS command 'dials.stereographic_projection hkl=0,0,1 expand_to_P1=True /path/to/dials/output/*refined.expt'

Note: It is a common pathology when processing stills data from crystals where the symmetry of the Bravais lattice is higher than the space group symmetry that merged data appear as a perfect twin. Data processing algorithms have ~~since adapted~~evolved to resolve ~~to~~ this pathology [43-46] but users should be mindful of this while processing their data.

~~This produces a plot with the central cross representing the beam direction and each point representing the direction of the hkl 001 reflection of individual lattices, with the outer ring of the circle representing a rotation of 90° away from the beam axis. This will show if your crystals have a preferred orientation, which may impact data completeness and indicate the need to collect more data or vary the loading protocol. In the left-hand panel of figure 7c, the effect of overloading a chip with HEWL crystals is shown. As apertures fill with more crystals they stick to the angled walls of the apertures rather than wedging at the base in a random orientation. The two orthogonal ellipses are a result of crystals lying on the internal walls of the chip which are at ~35° to the beam direction). Reducing the volume of crystals loaded reduces the hit rate but also dramatically reduces the fraction of crystals lying in these preferred planes.~~

REPRESENTATIVE RESULTS: (Instructions)

Low Dose Data Collection and Series

Low dose (5.1 Scenario 1) and dose series (5.2 Scenario 2) data were collected on copper nitrite reductase micro crystals at I24 and have been published in [42]. All samples were prepared as described in protocol section 1, data collected as per protocol sections 3, 4, and 5, and processed using methods in Protocols section 6. In this work a rapid dose series was collected with 20 diffraction images taken at each aperture (*i.e. n*=20 in the data collection GUI~~gui~~ shown above) before moving to fresh sample. From these data a bimodal distribution of unit cells in space group $P2_13$ was identified (a = b = c = 97.25 Å, and a = b = c = 96.38 Å). Identifying and separating these unit-cell polymorphs for processing showed a marked improvement in data quality indicators and revealed two different structures in a flexible loop between residues 189-193 instead of the mixed state observed when processing all data together. Identification of such polymorphs could make all the difference in a delicate time-resolved structural study where only small structural changes are expected. Furthermore, the dose series collected revealed a dose dependent unit cell change in the crystal, with increased dose shifting the population in favor of the larger unit-cell.

Similar work was performed in [47], where a dose series (5.2 Scenario 2) was collected from a dye-type heme peroxidase from *Streptomyces lividans* (DtpAa) to compare low dose structures from SSX (5.1 Scenario 1) with those measured in the same fixed target system using SFX. SFX data were collected at SACLA Beamline BL2 EH3 with a pulse length of 10 femtoseconds~~s~~ and a repetition rate of 30 Hz. The 10 femtoseconds~~s~~ pulse duration ensures that dose dependent

effects are not present in the SFX data. SFX data were compared to SSX data collected on beamline I24, where 10 sequential 10 milliseconds~~,~~ exposures were measured at each sample position (*i.e*. *n*=10). The dose dependent migration of a heme iron coordinated water molecule away from the iron was observed, as well as a conformational change in one of the heme propionate groups~~,~~ in the SSX dose series. Although not damage-free like the SFX structure, the dose series allowed the Fe-O_2H bond length of a zero-dose dataset (ferric heme) to be extrapolated, with this agreeing within experimental error with the value obtained from SFX.

The serial crystallography data collection methods described here can also be easily adapted to provide new sample environments to, for example, study anaerobic protein structures at room temperature. As outlined in [48], loading a 'sheet-on-sheet' sample, or 'chipless chip', with different sealing films in an anerobic chamber enables room temperature collection of structural data from dioxygen-sensitive samples.

Pump Probe

Although the following representative results were not collected at Diamond Beamline I24, these methods have been developed in close collaboration between facilities in the iNEXT program to work towards standard methods in serial crystallography method development. Beamline I24 offers, or will soon offer, equivalent collection methods to those used below already in the literature to perform such experiments using the methods described in the protocols above.

Pump Probe:~~—~~ Rapid Mixing

Rapid mixing SSX has been performed at beamline TREXX at PETRA III by [28] using a piezo driven droplet injector to initiate reactions on fixed targets. This work presents a proof of principle on chip mixing experiment binding $GlcNac_3$ to lysozyme microcrystals, with binding occurring within 50 ms of a 75 pl drop being applied to the sample. This study was followed up with a 7-structure time-resolved series of xylose isomerase activity, demonstrating glucose binding within 15 ms and the formation of an open ring conformation in the glucose molecule after a 60 second time delay. An equivalent setup for droplet injection is currently under development for use on I24.

Pump-Probe:~~—~~ Light Activation

A light activated pump-probe serial experiment is presented in [49]. Fluoroacetate dehydrogenase was soaked with photocaged fluoroacetate and pumped with 320-360nm laser light to produce structures at 4 time points (t=0, 30, 752, and 2,052 ms). The resting state structure (0 ms) shows an empty active site, with the exception of a few water molecules, and equivalent density between the cap domains of both protein subunits. 30 ms and 752 ms after light activation a significant reduction in electron density can be observed in the cap domain of subunit B relative to subunit A. The reduction in electron density in the cap domain of subunit B coincides with the appearance of fluoroacetate in the active site of subunit A at 752 ms. The final dataset at 2,052 ms shows further structural rearrangement of the ligand, suspected to facilitate the correct geometry for S_N2 attack, and potential formation of an intermediate state in the reaction. On

I24, a portable Pharos laser system which is tunable from 210-2500 nm providing femtosecond pulses can be used for light-activation. Initial experiments showed the successful activation of a photocage using 308 nm excitation with binding of the released ligand to the target protein observed. At the time of writing integration into the beamline personnel safety system is ongoing and routine user experiments are anticipated at the end of the year. For experiments when less intense pulses of light are required, light-activation with TTL controlled LEDs has been performed successfully.

FIGURE AND TABLE LEGENDS: (Instructions)

Figure 1: Sample loading equipment in place at Diamond Light Source, consisting of a vacuum pump (a), glove-box (b), and humidifier (c). Within the glove-box vacuum pressure is used to act on a chip loaded with crystal slurry held in a sample block (d) attached to a Büchner flask (e, green arrow), via a pressure regulator (f, yellow arrow) attached to a stopcock (g, blue arrow). Humid air is pumped into the tent via plastic tubing attached to the humidifier (h), and measured using a hygrometer (i). Components are held in place using clamp stands (j).

Figure 2: Sample holders utilise a metal O-ring (a) to clamp ~~mylar~~ polyester film onto a top (b) and bottom (c) half, with the bottom half sporting magnetic mounts (d) that are used to attach the sample holder to the sample stages. The ~~mylar~~ polyester film (6µm (e) or 3 µm (f)) as well as rubber O-rings (white arrows) prevent a crystal-loaded chip from drying rapidly in a sample holder which is closed tight with hex bolts (g). Chips are cleaned using sequential 15-minute baths in dH_2O, 1M HCl, and dH_2O (h).

Figure 3: Data collection GUI for fixed target data collection at I24. (a) shows the main interface used for aligning chips and defining data collection parameters, (b) is the mapping lite interface used for defining sub-regions of a chip for data collection and (c) is an interface for defining parameters for laser illumination.

Figure 4: The process of mounting a chip holder onto the stages as described in Protocol Section 3, point 1.

Figure 5: A chip is aligned by clicking on three fiducial markers on the chip shown in (a). Views of fiducials 0, 1 and 2 through the beamline on-axis viewing system are shown in (b), (c) and (d).

Figure 6: Auto-processing results displays launched as described in §6.1. An updating hit-rate plot is displayed (a, inset). If a 'hit' is clicked on the corresponding diffraction image is displayed in dials image viewer. The hit-rate for the current data collection is shown (29.6 % in this example) Panel (b) shows an example of a window showing current indexing and integration rates for data collected so far during the visit that updates in real time.

Figure 7: More in-depth data analysis. Visualisation of unit cell parameters can reveal polymorphs (a). Average unit cell parameters are calculated; however, this does not yet extend to individual averages for polymorphs. Visualisation of a small subset of data (data shown are a subset of 793

copper nitrate reductase crystals from the data described in Ebrahim *et al* 2019) is often sufficient to reveal trends. 2-D plots of useful parameters can also be produced to reveal variations that arise due to loading or dehydration effects that could be addressed for upcoming data collections (b). Stereographic projections can reveal the presence, or absence, preferred orientations feeding back into the loading protocol (c).

DISCUSSION: (Instructions)

Serial synchrotron data collection is a relatively new technique at MX beamlines, bridging the gap between the ultra-fast data collections currently being performed at XFELs and traditional synchrotron-based MX. This manuscript aims to give an overview of how to successfully collect fixed target serial data at beamline I24, Diamond Light Source for low dose, dose series, and time-resolved experiments. As with standard crystallography, sample preparation is a major bottle neck in structure solution. SSX is no different, and preparation of a homogenous crystal slurry in sufficient quantities has not yet benefited from several decades of study and refinement like the growth of single large protein crystals has. However, preparation of these slurries is outside the scope of this paper and has been summarized elsewhere[50] ~~(REF TO Beale)~~. The critical step in th~~is~~ approach~~protocol~~ described here involves the careful use of the available sample using easy to use GUI interfaces (§3) and ~~the available~~automated data processing pipelines (§~~described in protocols section~~ 6) to inform the chip loading (§1) and how an experiment should proceed~~in protocols section 1~~.

The fast feedback pipeline is a powerful tool that allows users to assess initial hit rates during data collection to inform subsequent chip loading protocols for successful data collection. When faced with a low hit rate (<5%), users risk collecting incomplete data and/or wasting beamtime with additional collections. In this case, sample could be pooled, concentrated by gentle centrifugation, and/or larger volumes could be loaded in step 1.5. A higher hit rate is generally favorable, however, there is a point of diminishing return where overloading leads to multiple crystals in the same well. DIALS is capable of dealing with multi~~ple~~ lattice diffraction data~~s to a point~~[51] ~~(REF????)~~, but a greater concern than indexing and integration is the detrimental effect crystal grouping ~~multiple crystals~~ can have~~be detrimental to~~ on the even activation of ~~a protein samples~~crystals by laser light or rapid mixing for precise time resolved experiments. ~~(JLME paper reference???).~~ Particular care are should therefore be taken to avoid overloading fixed targets for time resolved experiments.

The indexing and integration processing step produces a plot with the central cross representing the beam direction, each point representing the direction of the hkl 001 reflection of individual lattices, and the outer ring of the circle representing a rotation of 90° away from the beam axis. This will show if your crystals have a preferred orientation, which may impact data completeness and indicate the need to collect more data or vary the loading protocol. In the left-hand panel of figure 7c, the effect of overloading a chip with HEWL crystals is shown. As apertures fill with more crystals, they stick to the angled walls of the apertures rather than wedging at the base in a random orientation. The two orthogonal ellipses are a result of crystals lying on the internal walls of the chip which are at ~35°to the beam direction. This reduces the volume of crystals loaded,

Formatted: Font color: Red

reduces the hit rate, and dramatically reduces the fraction of crystals lying in these preferred planes.

Formatted: Centered

It should be noted that other serial approaches ~~(for example the LCP extruder)~~ are available at I24, such as LCP extruders and microfluidic chips~~4~~. These use similar GUIs and the same processing pipelines so much of the above will remain applicable even if a different technique is used. A number of serial approaches exist for both SSX and SFX beyond the fixed target approach described here, each has certain advantages over the other depending on the experiment you wish to perform and the beamline you are performing your experiment at. As serial approaches are evolving rapidly it is advisable to check the beamline webpages[1] for recent updates and talk to beamline staff at as early a stage as possible when planning beamtime. Access to I24 for standard and serial experiments is free at point of use. For UK and EU users travel and accommodation costs are partly covered through INEXT Discovery.

ACKNOWLEDGMENTS: (Instructions)
Enter text here.

DISCLOSURES: (Instructions)
Enter text here.

REFERENCES: (Instructions)

1. Schlichting, I., Serial femtosecond crystallography: the first five years. *IUCrJ* **2015,** *2* (2), 246-255.
2. Diederichs, K.; Wang, M., Serial Synchrotron X-Ray Crystallography (SSX). In *Protein Crystallography: Methods and Protocols*, Wlodawer, A.; Dauter, Z.; Jaskolski, M., Eds. Springer New York: New York, NY, 2017; pp 239-272.
3. Pearson, A. R.; Mehrabi, P., Serial synchrotron crystallography for time-resolved structural biology. *Curr Opin Struct Biol* **2020,** *65*, 168-174.
4. Chapman, H. N., Structure Determination Using X-Ray Free-Electron Laser Pulses. In *Protein Crystallography: Methods and Protocols*, Wlodawer, A.; Dauter, Z.; Jaskolski, M., Eds. Springer New York: New York, NY, 2017; pp 295-324.
5. Chavas, L. M.; Gumprecht, L.; Chapman, H. N., Possibilities for serial femtosecond crystallography sample delivery at future light sources. *Struct Dyn* **2015,** *2* (4), 041709.
6. Dauter, Z.; Wlodawer, A., Progress in protein crystallography. *Protein Pept Lett* **2016,** *23* (3), 201-10.
7. Owen, R. L.; Rudiño-Piñera, E.; Garman, E. F., Experimental determination of the radiation dose limit for cryocooled protein crystals. *Proc Natl Acad Sci U S A* **2006,** *103* (13), 4912-7.
8. Garman, E. F.; Weik, M., X-ray radiation damage to biological samples: recent progress. *J Synchrotron Radiat* **2019,** *26* (Pt 4), 907-911.
9. Axford, D., et al., In situ macromolecular crystallography using microbeams. *Acta Crystallogr D Biol Crystallogr* **2012,** *68* (Pt 5), 592-600.
10. Warren, A. J.; Axford, D.; Paterson, N. G.; Owen, R. L., Exploiting Microbeams for

[1] https://www.diamond.ac.uk/Instruments/Mx/I24.html

Membrane Protein Structure Determination. *Adv Exp Med Biol* **2016,** *922*, 105-117.
11. Sanishvili, R.; Fischetti, R. F., Applications of X-Ray Micro-Beam for Data Collection. In *Protein Crystallography: Methods and Protocols*, Wlodawer, A.; Dauter, Z.; Jaskolski, M., Eds. Springer New York: New York, NY, 2017; pp 219-238.
12. Wierman, J. L., et al., Fixed-target serial oscillation crystallography at room temperature. *IUCrJ* **2019,** *6* (2), 305-316.
13. Maeki, M., et al., Room-temperature crystallography using a microfluidic protein crystal array device and its application to protein–ligand complex structure analysis. *Chemical Science* **2020,** *11* (34), 9072-9087.
14. Grunbein, M. L.; Nass Kovacs, G., Sample delivery for serial crystallography at free-electron lasers and synchrotrons. *Acta Crystallographica Section D* **2019,** *75* (2), 178-191.
15. Weierstall, U., Liquid sample delivery techniques for serial femtosecond crystallography. *Philos Trans R Soc Lond B Biol Sci* **2014,** *369* (1647), 20130337.
16. Botha, S., et al., Room-temperature serial crystallography at synchrotron X-ray sources using slowly flowing free-standing high-viscosity microstreams. *Acta Crystallogr D Biol Crystallogr* **2015,** *71* (Pt 2), 387-97.
17. Kovácsová, G., et al., Viscous hydrophilic injection matrices for serial crystallography. *IUCrJ* **2017,** *4* (Pt 4), 400-410.
18. Monteiro, D. C. F., et al., A microfluidic flow-focusing device for low sample consumption serial synchrotron crystallography experiments in liquid flow. *Journal of Synchrotron Radiation* **2019,** *26* (2), 406-412.
19. Monteiro, D. C. F., et al., 3D-MiXD: 3D-printed X-ray-compatible microfluidic devices for rapid, low-consumption serial synchrotron crystallography data collection in flow. *IUCrJ* **2020,** *7* (Pt 2), 207-219.
20. Mueller, C., et al., Fixed target matrix for femtosecond time-resolved and in situ serial micro-crystallography. *Struct Dyn* **2015,** *2* (5), 054302.
21. Owen, R. L., et al., Low-dose fixed-target serial synchrotron crystallography. *Acta Crystallogr D Struct Biol* **2017,** *73* (Pt 4), 373-378.
22. Keedy, D. A., et al., Mapping the conformational landscape of a dynamic enzyme by multitemperature and XFEL crystallography. *Elife* **2015,** *4*.
23. de la Mora, E., et al., Radiation damage and dose limits in serial synchrotron crystallography at cryo- and room temperatures. *Proceedings of the National Academy of Sciences* **2020,** *117* (8), 4142-4151.
24. Barends, T. R., et al., Direct observation of ultrafast collective motions in CO myoglobin upon ligand dissociation. *Science* **2015,** *350* (6259), 445-50.
25. Pande, K., et al., Femtosecond structural dynamics drives the trans/cis isomerization in photoactive yellow protein. *Science* **2016,** *352* (6286), 725-9.
26. Standfuss, J.; Spence, J., Serial crystallography at synchrotrons and X-ray lasers. *IUCrJ* **2017,** *4* (2), 100-101.
27. Grünbein, M. L., et al., Illumination guidelines for ultrafast pump–probe experiments by serial femtosecond crystallography. *Nature Methods* **2020,** *17* (7), 681-684.
28. Mehrabi, P., et al., Liquid application method for time-resolved analyses by serial synchrotron crystallography. *Nature Methods* **2019,** *16* (10), 979-982.
29. Beyerlein, K. R., et al., Mix-and-diffuse serial synchrotron crystallography. *IUCrJ* **2017,** *4*

(Pt 6), 769-777.
30. Schmidt, M., Mix and Inject: Reaction Initiation by Diffusion for Time-Resolved Macromolecular Crystallography. *Advances in Condensed Matter Physics* **2013,** *2013*, 167276.
31. Kupitz, C., et al., Structural enzymology using X-ray free electron lasers. *Struct Dyn* **2017,** *4* (4), 044003.
32. Stagno, J. R., et al., Structures of riboswitch RNA reaction states by mix-and-inject XFEL serial crystallography. *Nature* **2017,** *541* (7636), 242-246.
33. Shilova, A., et al., Current status and future opportunities for serial crystallography at MAX IV Laboratory. *Journal of Synchrotron Radiation* **2020,** *27* (5), 1095-1102.
34. Huang, C.-Y., et al., In meso in situ serial X-ray crystallography of soluble and membrane proteins. *Acta Crystallographica Section D* **2015,** *71* (6), 1238-1256.
35. Gao, Y., et al., High-speed raster-scanning synchrotron serial microcrystallography with a high-precision piezo-scanner. *Journal of Synchrotron Radiation* **2018,** *25* (5), 1362-1370.
36. Beale, J. H., et al., Successful sample preparation for serial crystallography experiments. *J Appl Crystallogr* **2019,** *52* (Pt 6), 1385-1396.
37. Doak, R. B., et al., Crystallography on a chip - without the chip: sheet-on-sheet sandwich. *Acta Crystallogr D Struct Biol* **2018,** *74* (Pt 10), 1000-1007.
38. Axford, D.; Aller, P.; Sanchez-Weatherby, J.; Sandy, J., Applications of thin-film sandwich crystallization platforms. *Acta Crystallogr F Struct Biol Commun* **2016,** *72* (Pt 4), 313-9.
39. Davy, B., et al., Reducing sample consumption for serial crystallography using acoustic drop ejection. *Journal of Synchrotron Radiation* **2019,** *26* (5), 1820-1825.
40. Brewster, A. S., et al., Improving signal strength in serial crystallography with DIALS geometry refinement. *Acta Crystallographica Section D* **2018,** *74* (9), 877-894.
41. Winter, G., et al., DIALS: implementation and evaluation of a new integration package. *Acta Crystallographica Section D* **2018,** *74* (2), 85-97.
42. Ebrahim, A., et al., Resolving polymorphs and radiation-driven effects in microcrystals using fixed-target serial synchrotron crystallography. *Acta Crystallographica Section D* **2019,** *75* (2), 151-159.
43. Brehm, W.; Diederichs, K., Breaking the indexing ambiguity in serial crystallography. *Acta Crystallographica Section D* **2014,** *70* (1), 101-109.
44. White, T., Processing serial crystallography data with CrystFEL: a step-by-step guide. *Acta Crystallographica Section D* **2019,** *75* (2), 219-233.
45. Shi, Y.; Liu, H., EM-detwin: A Program for Resolving Indexing Ambiguity in Serial Crystallography Using the Expectation-Maximization Algorithm. *Crystals* **2020,** *10* (7), 588.
46. Gildea, R. J.; Winter, G., Determination of Patterson group symmetry from sparse multi-crystal data sets in the presence of an indexing ambiguity. *Acta Crystallographica Section D* **2018,** *74* (5), 405-410.
47. Ebrahim, A., et al., Dose-resolved serial synchrotron and XFEL structures of radiation-sensitive metalloproteins. *IUCrJ* **2019,** *6* (4), 543-551.
48. Rabe, P., et al., Anaerobic fixed-target serial crystallography. *IUCrJ* **2020,** *7* (5), 901-912.
49. Schulz, E. C., et al., The hit-and-return system enables efficient time-resolved serial synchrotron crystallography. *Nature Methods* **2018,** *15* (11), 901-904.
50. Beale, J. H., et al., Successful sample preparation for serial crystallography experiments. *Journal of Applied Crystallography* **2019,** *52* (6), 1385-1396.

51. Gildea, R. J., et al., New methods for indexing multi-lattice diffraction data. *Acta Crystallographica Section D* **2014,** *70* (10), 2652-2666.

Required formatting

- *File Type:* The manuscript must be submitted as an editable .doc or .docx file.
- *Font:* 12 pt, Calibri.
- *Line spacing:* Include single-line spaces between all paragraphs, headings, steps, *etc.*
- *Page margins:* 1 inch (2.54 cm) on all sides.
- *Page size:* Standard US Letter.

Technical Language

- The manuscript text must be **original, in complete sentences, and in paragraph form**.
- Define acronyms/abbreviations upon first use in the main text.
- Use SI abbreviations for all units: L, mL, µL, h, min, s, *etc.*
- Italicize all Latin words and nomenclature: *et al., in vivo, in vitro, in silico, i.e., e.g., etc.*
- Include a space between all numbers and the corresponding unit: 50 mg, 100 mL, 37 °C, *etc.*
- List all centrifugation speeds in terms of centrifugal g-force instead of rpm: 100 x g
- Molecular formulas should include subscripts: CO_2, H_2O_2, O_2, *etc.*
- Abbreviate species names after first use: *Caenorhabditis elegans* should be *C. elegans.*

TITLE: *(150 characters maximum)*
The title should represent the content included in the video and include the model system used or the type of study design. Please avoid the use of abbreviations.

AUTHORS AND AFFILIATIONS:

- Please provide full affiliations and institutional emails for all authors.
- Please see our Editorial Policies: (www.jove.com/author/editorial-policies) for more details regarding authorship.
- Affiliations should reflect where the work was performed. For multiple affiliations, use numerical superscripts.
- For equal contributions or other footnotes, indicate with an asterisk (*).
- The published corresponding author may differ from the one used for correspondence with the editorial office during the submission and publication process.

Please use this example as a model:
Jane A Smith[1], Edward A Jenner[1,2]
[1]Department of Biology, Harvard University, Cambridge, MA, USA
[2]Department of Neuroscience, Oxford University, Oxford, UK

Corresponding Author:
Edward A Jenner
EAjenner@ox.ac.uk

Tel: (978)-123-4567

Email Addresses of Co-authors:
Jane Smith (jasmith@harvard.edu)
KEYWORDS: *(6 minimum, 12 maximum)*

SUMMARY: *(10-word minimum, 50-word maximum)*
The summary should clearly state the goal of the protocol. It may include a general description of the method and its applications. This description should focus on the protocol, not the results obtained by the method.

ABSTRACT: *(150-word minimum, 300-word maximum)*
The abstract should focus on the method being presented rather than the results of a specific experiment. Include a statement about the purpose of the method. A more detailed overview of the method and a summary of its advantages, limitations, and applications is appropriate. Please focus on the general types of results acquired. Do not include references here.

INTRODUCTION: *(150-word minimum, 1500-word maximum, 2-paragraph minimum)*
This section should include:

- A clear statement of the purpose of this method
- The rationale behind the development and/or use of this method
- The advantages over alternative methods with references to relevant studies
- The context of the method in the wider body of published literature
- Information to help readers decide whether the method described is appropriate for them

PROTOCOL: *(1-page minimum, 10-page maximum)*
The protocol text should provide a detailed description to enable the accurate replication of the presented method (including setup, materials, actions, conditions, *etc.*) by both experts and researchers new to the field. Well-established methods (*e.g.*, Western Blotting, PCR, *etc.*) used within the protocol should be cited as necessary and any modification of the aforementioned procedures should be described.

A) Format:

- The protocol must be a numbered list: step 1 followed by 1.1, followed by 1.1.1, *etc*.
- Include a space between each numbered step or note in the protocol.
- Each step should include 1-2 actions and contain 2-3 sentences. Use sub-steps as necessary.
- Please do not use indentations.
- Do not underline any text in the protocol; however, **bold** text is acceptable for emphasis.

B) Grammar:

- Use complete sentences throughout the protocol.
- Avoid the use of personal pronouns or colloquial phrases (*e.g.*, I, you, your, we, our).
- Use the active/imperative voice throughout this section.

Good Example: Add 30 µL of solution A to 30 µL of solution B.
Bad Example: 30 µL of solution A was added to 30 µL of solution B.

- Avoid the use of commercial language, including ™/®/© symbols or company brand names before/after an instrument or reagent. Cite these in the Table of Materials instead.

C) Technical Specifications:

- Use subheadings for clarity if there are discrete stages in the protocol.
- Please indicate any points at which the experiment can be paused and then restarted later. For these situations, indicate the choices at that point in the protocol.
  Example: Incubate the filter for 4 h at room temperature or overnight at 4 °C.
- Indicate any toxic or harmful chemicals with the word "CAUTION" when they are first used, and include notes that describe the hazard and the appropriate handling guidelines.
- All methods that involve the use of human or animal subjects and/or tissue or field sampling must include an ethics statement before the numbered protocol section (see Editorial Policies: (www.jove.com/author/editorial-policies) for more information).

  Example: All methods described here have been approved by the Institutional Animal Care and Use Committee (IACUC) of Harvard University.

D) Protocol Length:

There is a 10-page limit (with proper formatting) for the amount of text written in the protocol section. There is a 2.75-page limit on the amount of content we can film for a single video article.

- **For a Protocol section that exceeds 3 pages, highlight in yellow up to 2.75 pages (no less than 1 page) of protocol text (including headers and spacing) to be featured in the video. Our scriptwriters will derive the video script directly from the highlighted text.**
  - Bear in mind the goal of the protocol, and highlight the critical steps to be filmed.
  - Please ensure that the highlighted steps form a cohesive narrative with a logical flow from one highlighted step to the next. The highlighted part of the step must include at least one action that is written in the imperative voice.
  - You do not need to delete steps from the protocol. The full-length manuscript will be published along with the video. All un-filmed steps will still be available in the written manuscript for readers.

E) Equations: (Example of JoVE video with equations: www.jove.com/51288)

- Ensure all inline equations are formatted identically, using the consistent font style.
- Separate each equation to its own line, and define all terms in the equation. A 4-line equation should take up 4x the vertical space as a single line equation.
- Do not embed equations as images. Instead, use the equation builder in MS Word.

F) Example Protocol:

1. Deactivation of Basic Alumina

1.1. To generate basic alumina (activity IV), add 100 g of basic alumina (activity I) to a 500-mL

round bottom flask.

1.1.1. Add 10 mL of water to the flask and fit it with a glass stopper.

1.1.2. Shake the flask vigorously until no lumps are visible, indicating even spreading of water throughout the alumina. Allow the alumina to cool to room temperature (RT).

CAUTION: Adsorption of water is exothermic, and the flask may get hot, which may result in a buildup of pressure. Release any pressure buildup frequently.

2. **Purification of the Iodoaziridine**

2.1. Purify the crude iodoaziridine by column chromatography using basic alumina (activity IV) as the stationary phase, eluting with hexane and grading to 5% EtOAc/hexane[7].

Note: High concentrations of EtOAc should not be used with basic alumina. In these cases, diethyl ether can be used instead.

2.2. Combine the product-containing fractions, and remove the solvent under reduced pressure to obtain the pure iodoaziridine.

Note: The protocol can be paused here.

REPRESENTATIVE RESULTS: *(Example Representative Results section: www.jove.com/52010)*
Please provide a concise, written description of a representative outcome following the use of this protocol, so that a viewer will have a sense of a "positive" and/or "negative" result. **Please reference all data and figures in the manuscript**, emphasizing how the results confirm the success of the protocol, and how to interpret the data. Please include data from successful experiments, and data from sub-optimal experiments to demonstrate the range of outcomes possible. Also include results for possible outcomes if critical steps are not followed. A diagram/schematic of the method is recommended but is NOT sufficient.

All claims of the effectiveness of a method must be supported with data, *i.e.*, representative results. For example: If authors claim that method X cleanly purifies nuclear envelope proteins from a cell, they must include a figure definitively demonstrating this purification. The manuscript must include at least one figure or table providing Representative Results.

Provide a separate file for each figure and table; do NOT embed figures or tables within the manuscript document. The default placement for all figures and results tables in the final publication is below the Representative Results text. Please indicate, via brackets [Place Figure 1 here], if you prefer figure/table placement at another location in the text.

If a figure is adapted or republished from a previous publication, authors must cite the original article in the figure legend. Reprint permission for the previously published/adapted figure is

required upon acceptance.

Example: This figure has been modified from [citation].[1]

FIGURES AND TABLES:

- Text: Use Calibri, 20 pt. font or greater.
- All figures should be provided as individual files. DO NOT embed them in the manuscript file.
- All microscopic images must include scale bars.
- All data figures must include measurement definitions and error bars (if applicable). Please define all error bars (SEM, SD, Range, *etc*.).
- Axis/Axis Tick Labels/Graph Lines: Use 20 pt. size font or greater, 3 pt. line weight or greater.
- A multi-panel figures (with parts A, B, C, *etc*.) should be submitted as a single, combined image file that contains all parts of the figure.
- Preferred figure file types: .eps, .psd, .pdf. Please save any .ai files as a .pdf for submission but maintain .ai files for production purposes.
- .tiff, and .jpg (not preferred) files must be at least 1,440 pixels x 480 pixels, or 300 dpi.
- Preferred animated figure file types: .mov, .mp4, .m4v (upload as "Animated/Video Figure").
- 50 MB maximum size (Contact your editor or submissions@jove.com for exceptions).
- All tables should be provided as individual .xls or .xlsx files and submitted as Tables.

TABLE OF MATERIALS:

A Table of Materials is required for all articles. A template is provided here. Please do not number the Table of Materials in the article. Please do not include any ™/®/© symbols here.

FIGURE AND TABLE LEGENDS:

Each figure or table, including supplemental figures/tables, must have an accompanying legend comprised of a short title and a short description of each panel or a general description. Legends should be included as part of the manuscript and not included in the figure file.

Example: **Figure 1: Representative flow cytometry analysis of non-permeabilized cells**. **A**. Schematic representation of gating strategy used in flow cytometry analysis sample. Data were analyzed after acquisition with the appropriate software… **B**. Semi-log graph for the….

DISCUSSION: *(3-6 paragraphs)*

JoVE is a methods-based journal. Thus, the Discussion section of the article should be focused on the protocol and not the representative results.

This section should discuss the following with citations:

- Critical steps in the protocol
- Modifications and troubleshooting of the method
- Limitations of the method
- The significance of the method with respect to existing/alternative methods
- Future applications or directions of the method

ACKNOWLEDGMENTS:

Please list acknowledgments and all funding sources for the work here. Also consider listing any person appearing in the film who does not appear in the authors list.

DISCLOSURES:

The corresponding author must ensure that all authors have disclosed any and all conflicts of interest. Examples of a conflict of interest would be "The author [full name] is an [employee/shareholder, *etc.*] of [full company name] that produces reagents and/or instruments used in this Article". If authors have no conflict of interest, a statement stating this must be included. The default text is "The authors have nothing to disclose."

REFERENCES *(10 minimum; if using EndNote, please use the JoVE EndNote style file)*

In-Text Formatting:

- The corresponding reference numbers should appear as superscripts after the appropriate statement(s) in the text (before punctuation but after closed parenthesis). The references should be numbered in order of appearance.
- Multiple references should be separated by commas, or a dash for inclusive numbers: example[2,5] refers to references 2 and 5, while example[2-5] refers to references 2 through 5.
- Personal communications, unpublished data, and conference abstracts can be cited parenthetically in the text with author last name, initials, and year.
- Footnotes should not be used. Grant details and personal acknowledgments should not be cited as a numbered reference (but included in the Acknowledgments section).

Citation Formatting: (in order)

- Last name, first and middle initials (if available). List ALL authors. If there are six or more authors, list the first author and then "*et al.*".
- Include article, book, or chapter titles. Titles of books should be italicized, whereas article and chapter titles should not.
- Article titles should start with capital letters and end with periods, and should appear exactly as they were published in the original work with no abbreviations or truncations.
- Write journal names in italics. The city or country where a journal is located can be included in parenthesis with the journal name. For books or other works, a publisher name, city, and country can be included.
- Write volume numbers in bold, followed by a space, issue number (in parentheses), a comma, and then a range of page numbers (start page – last page). A single page number or digital object identifier [doi] can be substituted for a range of page numbers.
- Provide the year published (in parentheses), followed by a period.
- "Accepted" or "In Press" can be listed after the title or journal name and before the year. Manuscripts that are in preparation or under review should not be listed.

Citation Examples:

Bedford, C.D., Harris, R.N., Howd, R.A., Goff, D.A., Koolpe, G.A. Quaternary salts of 2-[(hydroxyimino)methyl]imidazole. *Journal of Medicinal Chemistry*. **32** (2), 493-503 (1998).

Kioh, L.G. *et al. Physical Treatment in Psychiatry*. Blackwell Scientific Pubs. Boston (1988).